Abstract

After many years of fusion research, the conditions needed for a D-T fusion reactor have been approached on the Tokamak Fusion Test Reactor (TFTR). For the first time the unique phenomena present in a D-T plasma are now being studied in a laboratory plasma. The first magnetic fusion experiments to study plasmas using nearly equal concentrations of deuterium and tritium have been carried out on TFTR. At present the maximum fusion power is 10.7 MW, using 39.5 MW of neutral-beam heating, in a supershot discharge and 6.7 MW in a high-β_p discharge following a current rampdown. The fusion power density in the core of the plasma is $\approx$ 2.0 MW m^{-3}, exceeding that expected in the International Thermonuclear Experimental Reactor (ITER) at 1500 MW total fusion power. The energy confinement time, τ_E, is observed to increase in D-T, relative to D plasmas, by 20% and the $n_i(0)$ $T_i(0)$ τ_E product by 55%. The improvement in thermal confinement is caused primarily by a decrease in ion heat conductivity in both supershot and limiter-H-mode discharges. Extensive lithium pellet injection increased the confinement time to 0.27 s and enabled higher current operation in both supershot and high-β_p discharges. ICRF heating of a D-T plasma, using the second harmonic of tritium, has been demonstrated. First measurements of the confined alpha particles have been performed and found to be in good agreement with TRANSP simulations. Initial measurements of the alpha ash profile have been compared with simulations using particle transport coefficients from He gas puffing experiments. The loss of alpha particles to a detector at the bottom of the vessel is well described by the first-orbit loss mechanism. No loss due to alpha-particle-driven instabilities has yet been observed. D-T experiments on TFTR will continue to explore the assumptions of the ITER design and to examine some of the physics issues associated with an advanced tokamak reactor.

PACS Numbers: 28.52.Cx, 52.25.Fi, 52.55.Fa

I. INTRODUCTION

For nearly 40 years, fusion researchers have studied the confinement, heating and stability of hydrogen (H) and deuterium (D) plasmas while reactor designs were based on using deuterium-tritium (D-T) fuel [1,2]. Since December 1993 on TFTR, it has become possible to make a systematic study of the differences between D and D-T fuels. These studies are needed to validate the assumptions underlying reactor design such as that of ITER. During the past year, TFTR has created 280 D-T discharges with tritium concentrations up to 60%, ion temperatures (T_i) up to 44 keV, electron temperatures (T_e) up to 13 keV, fusion-power up to 9.3 MW, central fusion power densities to 2.0 MW m^{-3}, fusion-energy per pulse to 6.5 MJ. The experimental D-T program on TFTR [3] has significantly extended the limited-objective D-T experiments previously performed on JET which achieved 1.7 MW of fusion power with ~ 10% tritium fuel admixtures [4].

The principal goals of the TFTR deuterium-tritium experiments are:

1. Safe operation of the tritium handling and processing systems, and successful machine and diagnostic operation in a high radiation environment with 14 MeV neutrons;

2. Documenting changes in confinement and heating going from deuterium to tritium plasmas;

3. Evaluating the confinement of α particles, including the effect of α–induced instabilities, and measuring α heating, and helium ash accumulation;

4. Demonstrating the production of $\approx$10 MW of fusion power.

In this paper, a brief description will be given of the D-D experiments leading up to the D-T campaigns in TFTR. The optimization of the DT power within the constraints imposed by the available heating power, the energy confinement and the plasma stability are discussed.

Finally, the possibilities for further improvements in the DT fusion performance of TFTR are discussed and how they will address key design considerations of a tokamak reactor utilizing deuterium-tritium fuel.

The experiments described in this paper were conducted at a major radius of 2.45 to 2.62 m, toroidal field at the plasma center from 4.0 to 5.6 Tesla, and plasma current from 0.6 to 2.7 MA. Deuterium and tritium neutral beams with energies up to 115 keV were injected to heat and fuel the plasma with a total injected power up to 39.5 MW. ICRF power up to 8 MW has also been used. The plasma boundary is defined by a toroidal limiter composed of carbon-composite tiles in high heat flux regions, and graphite tiles elsewhere.

II. TRITIUM SYSTEMS AND OPERATIONS

Initial tokamak experiments at low tritium concentration were conducted in November 1993 and experiments at high tritium concentration began on December 9, 1993.

The tritium system on TFTR can handle concentrations of tritium from relatively low levels of ≈0.5% up to 100% and is run routinely with up to 5g of tritium (50 kCi) on site [5]. The tritium gas is brought on-site in an approved shipping canister and transferred to a uranium bed where it is stored. The uranium bed is heated to transfer the gas to the neutral beam or torus gas-injection systems. The gas is then injected into the torus or neutral beams and pumped by the liquid-helium cryo-panels in the beam boxes. During plasma operation, some of the gas is retained in the graphite limiter tiles in the vacuum vessel. The quantity of tritium in the vacuum vessel is restricted by PPPL requirements to 20 kCi. The gas on the cryo-panels is transferred to a Gas Holding Tank (GHT) for inventory measurement, and subsequently is oxidized and absorbed onto molecular sieve beds. These beds are shipped off-site for reprocessing or burial.

Since the start of D-T operation, 1.2×10^{20} D-T neutrons, equivalent to 340 MJ of fusion energy, have been produced. The activation of the vacuum vessel ~2 weeks after D-T operation is about 100 mrem/hr at vacuum vessel flanges, permitting limited maintenance and access to some machine areas.

In summary, the tritium processing systems are operating safely and are supporting the TFTR experimental run schedule. Operation and routine maintenance of TFTR during DT have been demonstrated. Shielding measurements have demonstrated that the number of D-T experiments will not be limited by either direct dose from neutrons and gammas or dose from the release of activated air or release of tritium from routine operations and maintenance.

III. TFTR MACHINE PERFORMANCE

TFTR experiments over the last 10 years have emphasized the optimization of high performance plasmas as well as studies of transport in high temperature plasmas. Figure 1 shows the progress of tokamaks in obtaining fusion power from DD and DT reactions for OH, NBI and RF heated plasmas. With increasing T_i and density, the fusion power from OH tokamaks steadily increased during the 1970's. With the advent of high power NBI in 1973, the fusion power was raised substantially relative to the OH plasmas of that time. Then finally in the 1990's, with D-T on JET and TFTR, the tokamak is producing substantial fusion power.

In TFTR the highest performance plasmas are supershots with peaked density profiles, which have performance, as measured by the parameter $n_i(0)T_i(0)\tau_E$, enhanced by a factor of ~ 20 over comparable L-mode plasmas, or a factor of ~5 over standard H-mode plasmas with a broad density profile. The enhanced confinement of supershots is correlated with the peaking of the density profile, $n_e(0)/\langle n_e \rangle$. In plasmas with constant beam power, the confinement enhancement over L-mode rises to ~3 as $n_e(0)/\langle n_e \rangle$ increases to 3**{Ref. Meade or Park}** An important feature of the supershot regime is that the confinement

time does not decrease with heating power, in contrast to L-mode and H-mode plasmas where $\tau_E \sim P_{heat}^{-1/2}$. This feature is also evident in the local transport coefficients for supershots and L-modes, and suggests that the basic mechanism causing transport is substantially modified in supershots relative to L-mode plasmas.

During the past year, as a result of extensive wall conditioning with lithium pellets [6], supershots have been produced at $I_p = 2.7$ MA corresponding to $q_\psi = 3.8$. This represents a significant extension of the supershot regime from plasma currents of 2.0 to 2.7 MA. Typically, 2 Li pellets (~ 2 mm diameter) are injected into the plasma in the ohmic phase of a pulse prior to beam injection, and 2 Li pellets are injected into the post beam injection ohmic phase in preparation for the next discharge. Each pellet deposits approximately one monolayer of Li on the vacuum vessel first wall. This conditioning results in energy confinement time which increased from typically 160 ms to a maximum of 270 ms in D-T plasmas. For the first time, the fusion performance of TFTR at the highest beam power and plasma current is not limited by plasma energy confinement, but rather by stability near the beta limit.

IV. FUSION POWER

TFTR has an extensive set of fusion neutron detectors (5 fission detectors, 2 surface barrier detectors, 4 activation foil stations, a collimated scintillating fiber detector [7], and a 10 channel neutron collimator with 25 detectors) to provide time and space resolution as well as energy discrimination of the D-T and D-D neutron fluxes [8]. The systems were calibrated *in situ* by positioning an intense DT neutron generator source at many locations within the vacuum vessel. In addition, the activation system is absolutely calibrated by neutronics modeling of the neutron scattering. The yield measured by the fission, surface barrier and ^{4}He recoil detectors is linear with measurements by activation foils over 6 orders of magnitude. The system of multiple measurements and calibrations has allowed

high accuracy, ± 7%, determination of the fusion energy production. Neutron-emission profiles which is peaked in the center of the plasma are measured by the neutron collimator.

As shown in Fig. 2, the highest fusion power of 9.3 ± 0.7 MW was achieved in a supershot discharge at I_p = 2.5 MA. The highest fusion power in a current rampdown (high-β_p) experiment was 6.7 MW achieved in a 1.5 MA discharge.

Figure 3 shows the time evolution of the DT fusion power from a sequence in Dec. 1993, May 1994 and Nov 1994, leading up to the shot producing the highest instantaneous power of 10.7 MW at 39.5 MW of input power for an instantaneous Q of 0.27. Q is defined as the instantanous total fusion power divided by the total injected NBI power, shine-through, first-orbit loss, dW/dt terms, etc are not subtracted from the total injected NBI power and each DT fusion is counted as giving 17.6 MeV of energy. Normally the neutral beam heating pulse length is limited, typically to 0.7 - 0.8 s, to reduce neutron activation of the tokamak structure. In this sequence, the neutral beam power and the amount of lithium conditioning were progressively increased. Only shots with tritium NBI are shown in Fig. 3; shots with deuterium NBI only were interspersed between the tritium shots for conditioning of the walls. The final shot in the sequence disrupted after 0.44 s of NBI when exceptionally good confinement increased the plasma pressure above the beta limit. The Troyon-normalized-β, β_N ($=10^8\beta_T a B_T/I_p$ where β_T is the total toroidal β and a is the plasma minor radius) reached 1.9 or 2.3. The parameter of relevance for fusion yield is $\beta_N^* \equiv 2\mu_o \langle p^2\rangle^{1/2}$ a (m)/[Ip (MA) $\bullet B_T$ (T)], where $\langle p^2\rangle^{1/2}$ is the root-mean-square plasma pressure, which reaches 3.0 for this plasma. Values of β_N = 3.0 with β_N^* = 4.2 have been achieved in high fusion power discharges in which the current was ramped down (for profile control purposes.) from 2.5 to 1.5 MA.

The measured neutron emission profiles agree well those calculated by TRANSP using measured plasma parameters as shown in Fig. 4 **[new Ref. 9 = old Ref. 14].** The beam voltage is approximately 105 keV for the case shown. The beam neutrals are injected

with full, half, and third energies. The fractions of the neutral currents at full energy is 0.49 for tritium and 0.43 for deuterium. The fractions at half energy is 0.38 for tritium and 0.39 for deuterium. The neutron emission is due to beam-thermal, beam-beam, and thermonuclear reactions. The separation between these reactions is discussed in **[new Ref. 10 = R.V. Budny, Nucl. Fusion 34 (1994) 1247].**

V. TRANSPORT AND CONFINEMENT IN D-T

1.0 Tritium Particle Transport.

Tritium operation in TFTR [9,10] has provided a unique opportunity to study hydrogenic particle dynamics in reactor relevant plasmas. The enhancement factor of ≈ 100 in DT neutron cross section, compared to that for DD reactions, allows easy diagnosing of both trace tritium particle transport and influx from the limiter. To study differences in particle transport between deuterium and tritium, experiments were performed with small concentrations of tritium prior to the walls becoming loaded with tritium. These experiments entailed the use of either deuterium containing a trace tritium concentration (<2%) or small puffs of pure tritium gas puffing into a deuterium beam heated discharge. These experiments showed relatively rapid radial tritium transport such that the effective tritium particle confinement time $\tau_{p(T)}$ is approximately equal to the energy confinement time τ_E and that the tritium particle transport coefficients are comparable to He particle transport coefficients in similar deuterium plasmas**[Ref. 10A].** Figure 5 shows the tritium transport coefficients, $D_T(r)$ and $V_T(r)$, as determined from multiple regression analysis. In addition, the transport coefficients of ^{4}He measured by charge-exchange recombination spectroscopy on similar plasma discharges are shown for comparison [11]. Also included in the plot is the deuterium thermal conductivity determined from equilibrium power balance analysis. The diffusivities are all similar in magnitude and profile shape: $D_T \sim D_{He} \sim \chi_D$. The similarity of the diffusivities has been observed in previous perturbative

transport experiments on TFTR and is a prominent characteristic of transport due to drift-like microinstabilities [11-13]. In addition, the similarity in the diffusivities has been shown to be attractive with regard to helium ash removal for future reactors, such as ITER [11].

In both the tritium gas puffing and in the subsequent high power deuterium-tritium neutral beam heating experiments, spectroscopic measurements have shown that the influx of tritium from the limiters is relatively small (<5%) and that the edge fueling from the limiter is predominantly deuterium. The relatively rapid transport to the core together with the relatively low influx of tritium from the walls affects the ratio of n_D/n_T in the plasma core. The thermal tritium density in the core of deuterium-beam-fueled discharges, from neutron emission measurements, shows that the nT/nD ratio decreases by a factor of 2.5 because of influx from the wall to the core due to the beam fueling.

2.0 Isotope Effects in Supershots

The experiments performed in December 1993 and May 1994 provided a clear demonstration that the plasma confinement in D-T supershots is better than in similar D-only plasmas, as shown in Fig. 6. The plasma energy is determined from magnetic data and includes the energy in the unthermalized injected deuterons and tritons. These plasmas were generated using co and counter tangential neutral beam injection (15-30 MW) into low edge-recycling plasmas, with plasma currents of 1.6 - 2.5 MA. The stored plasma energy, electron, and ion temperatures increased in deuterium-tritium plasmas compared with similar deuterium plasmas, corresponding to an increase in τ_E from 160 ms to 200 ms and in the product $n_i(0)\ T_i\ \tau_E(0)$ from 1.9 x 10^{20} to 3.5 x $10^{20} m^{-3}$ keV-s. The energy confinement time in these supershot discharges increased with the average mass of the hydrogenic ions as shown in Fig. 7. This improvement in thermal energy confinement with ion mass is observed for both supershots [14,15] and limiter H-modes [16] in TFTR. The ion temperature and electron density profiles for an Ip = 1.6 MA plasma with 8 MW

of tritium and 8 MW of deuterium NBI are shown in Fig. 8. There is a 20 - 30% increase in $T_i(0)$ and only a 5 - 10% increase in the $n_e(0)$ going from D-D to D-T plasmas.

There are a number of expected differences between T- and D-neutral beam heating, which are modeled using the SNAP and TRANSP codes. For T-NBI, the beam deposition profile is broadened, the beam heating of thermal ions is increased and the heating of electrons is decreased. The fusion generated alpha particles are expected to primarily heat the electrons. Taken together, these effects tend to cancel, producing small net changes in the total ion or electron heating powers when changing from D- to T-NBI in the plasmas studied. The power balance analysis indicates that the higher T_i gradient measured during a 50/50 D-T plasma relative to a pure D plasma is due to a reduction of the ion thermal diffusivity χ_i^{tot} by a factor of 2 for r/a $\leq$0.5 (Fig. 9). The lack of substantial change in the density gradient, despite the broader beam deposition profile with T-NBI, indicates a drop in the core electron particle diffusivity D by ~30%.

The limiter H-modes produced on TFTR in high-β_p D-T plasmas [17] have energy confinement enhancements > 4 relative to the ITER-89P scaling [17] while corresponding D plasmas had enhancements of ~3.2. The confinement was improved across the plasma during the H-mode phase. In particular, the ion heat conductivity was observed to decrease by a factor of 2 - 3 across the transition to H-mode[17] (Fig. 10). The edge localized modes (ELMs) are much larger during the D-T H-modes. This suggests that ITER D-T plasmas may be more susceptible to giant ELMs than inferred from D-only experiments. The power threshold for the transition to an H-mode is similar in D and D-T discharges [18].

One focus of the present experimental campaign is the turbulence and transport characteristics of D-T plasmas which have indicated improved ion confinement properties during D-T operation. Initial results from BES indicate that there appears to be a reduction in the local $\tilde{n}/n$ in D-T plasma compared to similar D-D cases (Fig. 11). An extensive

study of isotope scaling effects on confinement and fluctuations is planned for the near future.

VI. α–CONFINEMENT AND α-HEATING

1.0 Effects of Alpha Particles

The behavior of alpha particles from D-T reactions is a fundamental consideration for the performance of a future D-T reactor for two reasons. First, if a significant fraction of the alpha particles is not confined, then the confinement requirements for ignition would increase. Second, if a small unanticipated fraction (a few percent) of the alpha particles are lost in ITER, and the resulting heat flux is localized, damage to first-wall components could result. The heat load on the vessel components from alpha particles is due to a combination of classical effects associated with high-energy particle orbits in the inhomogeneous magnetic field, and instabilities in the plasma resulting in a loss of alpha particles. The operating point for a reactor is determined in part by the confinement of alpha particles, the transfer of energy from the alphas to the background plasma, and the accumulation of low energy alpha ash in the plasma which displaces the deuterium and tritium ions. TFTR experiments are aimed at studying this broad range of alpha particle physics and documenting them for conditions relevant to the reactor regime.

2.0 Single-Particle Effects

An extensive study of fusion product losses in deuterium experiments had been conducted prior to beginning D-T experiments [19]. During the D-T experiments the scintillator probes located at 90°, 60°, 45°, and 20° below the outer midplane detect alpha particle losses. The results from the 90° detector during D-T (shown in Fig. 12) match the first orbit loss model in both magnitude and pitch angle distribution. For detectors closer to the midplane, the first orbit loss model does not adequately fit the losses from D-D or D-T

plasmas. Collisional and stochastic toroidal field ripple losses are being investigated to explain the pitch angle distribution observed there.

These probes are also used to study the effect of ICRF on energetic particles. In a deuterium-tritium plasma, the alpha particle losses are observed to increase with the application of ICRF as shown in Fig. 13. The magnitude of the increase in loss is small (<50% of the first orbit loss which corresponds to ≈ < 3% of the total alpha birth rate) but clearly visible on the probes. The same effect is also seen in DD plasmas, for DD fusion products. The present understanding is that the ICRF, which primarily increases the $v_\perp$ of the resonant particles, heats the alpha particles and a part of the population crosses the passing-trapped boundary and enters the first orbit loss cone, resulting in increased loss [20].

3.0 Alpha Heating.

The electron heating in D-T supershot plasmas has been analyzed for evidence of heating by fusion-produced alpha particles. During the NB-heated phase of the discharge, the alpha heating contributes ~ 1 MW out of ~ 10 MW of heating power to the electrons, making its detection difficult. The first method of detecting alpha heating is to analyze and simulate the steady-state power balance of the electrons. Simulations using the measured plasma parameters (except T_e), and the χ_e experimentally inferred from the deuterium-comparison discharge indicate that alpha heating may be responsible for about half of the observed 2 keV increase in T_e going from D to D-T plasmas. The second method is to examine the transient response of the elections to a sudden change in the alpha heating. In a pair of nominally identical D and D-T plasmas, a lithium or boron pellet was injected ~0.2 s after the termination of NBI. The initial density increase and T_e decrease upon injection of the pellets were nearly identical in the two cases. By the time of pellet injection, most of the circulating beam-ions have thermalized, but the alpha particles have not due to their longer slowing down time. In addition, much of the tritium in the plasma is calculated to

had been pumped out of the plasma by the conditioned graphite limiter. The T_e reheat rate after pellet injection for the condition discussed above is measured to be ~85% higher in the D-T plasma relative to the D plasma, in agreement with TRANSP calculations of the expected alpha heating of the electrons. Additional experiments at higher alpha particle densities and pressures are planned.

VII. CONFINED ALPHA MEASUREMENTS

The first experimental results have been obtained with two of the new alpha particle diagnostics of confined alphas from D-T reactions. The alpha-charge exchange diagnostic obtained data during ablation of a Li pellet fired into a 2.5 MA D-T plasma, after the neutral beams were turned off. In the case shown in Fig. 14, the different analyzer energy channels give an energy spectrum of the alphas in the plasma core in the range 2 MeV down to 0.5 MeV. The measured shape of the energy spectrum of the alphas is in good agreement with a TRANSP calculation, although an absolute calibration of the diagnostic is not yet available. Charge-exchange-recombination-spectroscopy has been used to measure the alpha particles with energies up to 600 keV in a D-T pulse soon after the T-beams have been turned off, but with D-beams remaining on to allow the measurement. The signal predicted from the alpha distribution function calculated by the TRANSP code is within a factor of two agreement with the measured absolute intensity, demonstrating that this technique can be used to make absolute measurements of the alpha density. Further work is in progress to evaluate the effects of stochastic ripple diffusion and sawtooth oscillations on the alpha energy and radial distributions and to compare them quantitatively with theory.

VIII. α–ASH ACCUMULATION

The production, transport, and removal of helium ash is an issue that has a large impact in determining the size and cost of ITER. The present experiments on TFTR are providing the first opportunity to measure helium ash buildup, assess helium transport coefficients, and examine the effects of edge helium pumping on central ash densities in D-T plasmas. In

addition, the importance of the central helium source in determining the helium profile shape and amplitude is being examined.

Initial measurements of radial ash profiles have been made using charge-exchange recombination spectroscopy. Differences between similar D-D and D-T supershots in the time history and amplitude of the thermal helium spectrum enables the alpha ash profile to be deduced. These measurements have been compared to predictions from the TRANSP code, using transport coefficients from earlier helium puffing experiments in deuterium plasmas and the TRANSP calculation of alpha particle slowing-down and transport upon thermalization. The ash profiles are consistent with the TRANSP modeling, indicating that the ash readily transports from the central source region to the plasma edge and recycles. These measurements provide evidence that, in the presence of a central helium ash source, the ash transport and confinement time are roughly consistent with external helium gas puffing measurements. This suggests that helium transport in the plasma core will not be a fundamental limiting factor for helium exhaust in a reactor with supershot-like transport. Further dedicated experiments will be performed to determine the alpha ash particle transport coefficients in D-T plasmas.

IX. MHD STABILITY IN D-T PLASMAS

1.0 MHD Activity in the initial TFTR D-T plasmas

Low m and n (m/n = 2/1, 3/2, 1/1, etc.) coherent MHD modes have been observed in the initial D-T plasmas on TFTR. The amplitude, frequency of occurrence and effect on plasma performance are similar to those observed in comparison D-only plasmas. Modeling of the effect of MHD on confinement suggests that the MHD can be responsible for up to a 30% decrease in the energy confinement time in the worst cases [21], consistent with the observations. In cases of weak MHD, typical of most of the higher current plasmas (I_P > 2.0 MA, q_{sh} < 4), the effect is usually less than 5% (Fig. 15). The decrease in neutron rate is consistent with the changes in the equilibrium plasma: it is not necessary to invoke

anomalous losses of fast beam ions to explain this decrease. Enhanced losses of fusion α's, correlated with the presence of MHD, are observed in DT plasmas. The losses are similar to those previously reported for DD plasmas [22], and represents a small fraction of the total alpha population..

Fishbone and sawtooth activity have also been observed in D-T plasmas. At present there is no evidence that the fusion α's have affected the sawtooth or fishbone stability. There is a tendency for the fishbone activity to be stronger in D-T plasmas; however, that may be more correlated with the somewhat broader pressure profiles often found in D-T plasmas, as compared to D-only plasmas under similar conditions.

2.0 β limit and disruptions in D-T plasmas

Currently, the DT fusion power which TFTR can produce is limited by pressure driven instabilities which can cause major or minor disruptions. The disruptive β-limit in D-only NBI heated plasmas and D-T NBI heated plasmas appears to be similar. The β-limit follows approximately the dependence on plasma current and magnetic field predicted in the Troyon formula [23]. The high β disruption in D-only or D-T plasmas appears to be the result of a combination of an n=1 internal kink coupled to an external kink mode and a toroidally and poloidally localized ballooning mode [24]. Figure 16 shows contour plots of the electron temperature measured at a 500 kHz sampling rate by the two ECE grating polychromators (GPCs) separated by 126° in the toroidal direction. The ballooning character of this mode is observed as a poloidal asymmetry on the magnetic loop signals, the signal is 5 times larger on the outside than the inside. The simultaneous presence of the ballooning mode on one GPC, and its absence on the second clearly demonstrates the toroidal localization of the mode. The ratio of the frequency of the ballooning mode and the n=1 kink indicate that the ballooning mode has a toroidal wave number of about 10-15 (assuming only toroidal rotation). The radial structure of the kink mode suggests coupling of a predominantly internal kink to a weaker external kink. While PEST [25] predicts that

the n=1 kink is unstable for this disrupting plasma, it also in general predicts that most supershot plasmas are similarly unstable, as q(0) is typically less than unity [26] and the plasma pressure is sufficient to drive an ideal mode.

The kink mode can locally decrease the magnetic shear and increase the local pressure gradient so that the ballooning mode is locally destabilized. The thermal quench phase may result from destruction of flux surfaces by the non-linear growth of the n=1 kink, possibly aided by the presence of the ballooning modes. There is no evidence for a global magnetic reconnection as is seen in high density disruptions. The electron temperature collapses on a time scale of several hundred microseconds with no local flat spots, indicating that the magnetic geometry is destroyed uniformly over the plasma cross-section. The thermal quench phase is typically preceded by a large non-thermal ECE burst. The burst is at least 10 to 20 times larger in amplitude than is predicted by the fast compression of electrons by a rapidly growing internal kink displacement [27].

In both D and D-T experiments, MHD activity with low toroidal and poloidal mode numbers is observed to increase the loss of fusion products. Both minor and major disruptions produce substantial losses of alpha particles. In a major disruption, ~ 20% of the alpha stored energy is observed to be lost in ~2 msec during the thermal quench phase, while the plasma current is still unchanged. The loss is preferentially to the bottom of the vessel (90° with respect to the midplane), which is in the ion ∇B-drift direction, as opposed to locations such as 20°, 45° or 60° below the midplane where the other alpha particle detectors are located. The design of in-vessel components in a reactor will have to accommodate the localized heat flux from alpha particles during a disruption.

3.0 Toroidal Alfvén Eigenmodes studies

Experiments on TFTR [28] and DIII-D [29] have demonstrated that it is possible to destabilize the Toroidal Alfvén Eigenmode (TAE) with neutral beams and ICRF tail ions. In both cases, there is some loss of energetic beam particles and tail particles. Two of the

most important physics questions are whether alpha-induced instabilities are present and whether the predicted thresholds are in agreement with the experiment.

The highest fusion power shots on TFTR have produced fast α populations with some dimensionless alpha parameters, such as $R\nabla\beta_\alpha$, which are comparable to those for the projected fast α populations for ITER. In typical TFTR D-T supershots, the thermal and beam ion Landau damping are stronger than the fusion-α drive for TAE modes. Experiments were done successfully to reduce the thermal ion Landau damping; however, the α-drive was still not sufficient to overcome the beam ion Landau damping [30,31].

At fusion power levels of 7.5 MW, fluctuations at the Toroidal Alfvén Eigenmode frequency were observed with various fluctuation diagnostics to increase. However, no additional alpha loss due to the fluctuations was observed. Figure 17 shows that the fraction of alpha particles that are lost is independent of the fusion power, indicating that additional loss does not occur at high power up to 9.3 MW.

The threshold for instability is determined by a balance between drive and damping terms. Recent experiments have investigated modifying the relationship to test the theory quantitatively. For TFTR parameters, electron and ion Landau damping can be important. In one series of experiments at relatively high fusion power (5 MW), the ion temperature was suddenly decreased by employing a He gas puff, or injection of a Li or D_2 pellet. This rapidly decreased the central ion temperature from 22 keV to 6 keV. Despite the change in electron and ion Landau damping, the mode was not destabilized. A more detailed analysis is in progress to compare theory and experiment.

Experimentally the search for α-driven TAE activity in D-T plasmas has been complicated by the presence of a mode near the expected TAE frequency in both D-D and D-T NBI heated plasmas. This mode has a relatively broad peak in frequency, with a spectral width of about 50 kHz at 300 kHz. This mode may represent a 'thermal' level of excitation or be

driven by fast beam ions. For these plasmas the beam ion velocity is one third to one fifth the Alfvén velocity [32].

In Fig. 18 is shown the spectrum of the edge magnetic fluctuations for a D-T shot with 7.5 MW of fusion power and for a similar shot at 6.5 MW and a D-only shot. The mode amplitude has increased by a factor of 2 - 3 in the 7.5 MW shot. The NOVA-K code [33] finds n=5 and n=6 core-localized TAE activity in the region where $q<1$ in this plasma [34]. The localization of the mode near the plasma core increases the coupling of the fusion α's which makes the mode unstable. The calculated TAE mode frequency from the NOVA code was about 250 kHz, lower than the experimental frequency of 300 kHz. In this experiment the toroidal mode number was not measured.

X. ICRF HEATING IN D-T

In preparation for D-T operations, the TFTR ion cyclotron range of frequencies (ICRF) heating system has been upgraded. The positions of the antennas can be controlled remotely to maximize coupling to the plasma in different regimes. Phasing of the antennas at 0°, 180°, and 90° has been established in both deuterium majority and ^{4}He plasmas to allow for both heating and current drive studies. The antennas have operated successfully during D-T plasmas. The increased radiation field from D-T neutrons, as well as the β-decay from tritium, has not affected antenna performance.

ICRF wave physics in deuterium-tritium plasmas is complicated by the possibility of multiple, spatially separated resonances and by alpha damping which can compete with electron absorption in the fast-wave current-drive regime. A promising scenario for heating D-T plasmas is fast wave absorption at the second harmonic of the tritium cyclotron frequency, which is degenerate with the ^{3}He fundamental. By selectively heating a majority ion species rather than a minority ion species, potential difficulties with instabilities (e.g., TAE modes) excited by fast ions may be avoided. Though the core damping is predicted to be acceptable, off-axis absorption near the deuterium fundamental

and n^2=S layers can compete with the second harmonic tritium core damping in tokamaks with moderate aspect ratio. In TFTR supershot plasmas, with the second harmonic tritium heating ($2\Omega_T$) layer coincident with the Shafranov-shifted axis at 2.82m, the second harmonic deuterium and fundamental hydrogen heating ($2\Omega_D$ / Ω_H) layer is out of the plasma on the low field side, but the fundamental deuterium heating (Ω_D) layer is in the plasma on the high field side at R ~ 2.1m.

Experiments have been performed utilizing combined ICRF heating and neutral beam injection in deuterium-tritium plasmas. The initial experiments have focused on the RF physics associated with D-T plasmas. Second harmonic tritium heating with a 2% ^{3}He minority at a power of ~5.5 MW in a plasma with 23.5 MW of neutral beam injection (60% in T) has resulted in an increase of the ion temperature from 26 to 36 keV. The electron temperature increased from 8.5 to 10.5 keV due to direct electron damping and ^{3}He minority tail heating (Fig. 19). Similar heating was measured in discharges in which no ^{3}He was added. These favorable results indicate that ICRF can be used to heat a D-T plasma with core second-harmonic tritium damping. The observed second-harmonic tritium damping is consistent with 2D code predictions (Fig. 20), but the observed off-axis fundamental D damping is much less than the 2D code estimate. Further analysis of the power deposition in both deuterium and deuterium-tritium experiments is in progress.

Experiments using a ^{3}He, ^{4}He, D ohmic target plasma have shown localized electron heating near the mode conversion surface where excitation of the Ion Bernstein Wave (IBW) is predicted. Localized off-axis power deposition centered at $r/a < 0.25$ with half-width $\Delta r/a < 0.17$ has also been observed. Up to 75% of the radio frequency power is observed to be deposited on electrons. Numerical modeling indicates that 74-91% of the power should be damped on electrons, with the remainder damped on ions [35].

Majeski et al. [36] have suggested that this mode-converted ion Bernstein wave excited at the n^2 = S mode conversion layer in a multiple ion species plasma (such as D-T) could be

used for electron heating or to drive localized electron currents. Preliminary experiments to investigate mode conversion current drive (MCCD) in ^{3}He-^{4}He plasmas and fast wave current drive in ^{4}He(H) plasmas have begun. Initial results from the MCCD experiments show a strong dependence of the electron response on the direction of the launched waves. In this experiment, comparisons were made between similar shots with the waves launched either parallel or anti-parallel to the plasma current. For these comparison shots the loop voltage, electron density, and visible bremsstrahlung were identical. In contrast, for the FWCD case, the loop voltage depends on the direction of the RF wave propagation. The change in loop voltage during FWCD corresponds to ≈40 kA of RF driven currents. FWCD or MCCD techniques could play a crucial role in advanced tokamak regimes for TPX and ITER.

XI. ADVANCED TOKAMAK OPERATION IN D-T

Experiments on TFTR have demonstrated the benefits of advanced tokamak regimes characterized by a strongly peaked electron density profile, $n_e(0)/\langle n_e \rangle \leq 3.4$ (central density divided by the volume averaged density), and by large ratios of $\tau_E/\tau_E(\text{L-mode}) \leq 4.5$ along with $T_i/T_e < 4$ — resulting in high fusion power. As shown in Fig. 2, the 2.0 MA L-mode discharges produce much lower fusion power than comparable supershots or high-β_p discharges. Both the supershot and high-β_p regimes have large bootstrap current fractions which reduce the requirements for current drive, an attractive feature for reactors. Values ranging up to 70-80% have already been achieved in deuterium plasmas on TFTR. To take full advantage of these advanced-tokamak features calls for control of the current and pressure profiles so as to optimize the plasma reactivity while also maintaining plasma stability. The current profile was modified in both the high-βp experiments and in experiments that produce a region of reversed shear near the plasma core, resulting in favorable global and central confinement. These experiments also result in increased values of q(0), which could destabilize the TAE in D-T experiments [37]; however, at sufficiently high values of β the TAE instabilities are expected to become stable again [38]. Thus, the

path to a desirable D-T tokamak reactor regime may turn out to be rather complex; not only must the plasma maintain overall stability but also stability against TAE modes.

The highest fusion powers on TFTR, JET, JT-60U and DIII-D have been achieved in hot-ion mode experiments, with $T_i > T_e$. For reactor plasmas, Clarke [39] has shown that the hot-ion mode could be achieved if $\chi_i << \chi_e$ or the alpha energy were transferred directly to the ions. In TFTR L-mode experiments, $\chi_i > \chi_e$; however, in supershots and in high-βp experiments with H-mode transitions, TFTR obtains $\chi_i < \chi_e$ in its reacting plasma core. Recently, Fisch and Rax [40] have pointed out that by coupling the α-power to a plasma wave that is damped by thermal ions, it may be possible to channel a significant fraction of the alpha energy to the ion channel. Such an approach would serve also to decrease the energy stored in the electrons and alphas — thus permitting an increase in the ion stored energy and thereby potentially doubling the plasma reactivity at fixed β_t. By appropriately choosing the wave, it may also be possible to drive the plasma seed current. D-T operation in advanced tokamak regimes introduces both new experimental challenges associated with coupling the free alpha-particle energy to plasma instabilities as well as opportunities to harness the alpha-energy for the improvement of the tokamak reactor concept.

XII. SUMMARY

Tritium and neutron activation are being handled safely, thereby allowing TFTR to operate a full schedule and to be maintained routinely. TFTR presently plans to run most of FY95, based on present funding, and expects to stop operation in September 1995.

The D-T experiments on TFTR have allowed the direct examination of many critical issues of physics and technology for ITER, and has clarified what new technical features could be most helpful to an advanced tokamak reactor. The confinement in a D-T plasma in TFTR is better than in a D-D plasma, allowing significantly improved $n\tau T$ fusion performance in D-T. The alpha particles are found to be confined as expected and hints of alpha heating have already been seen. ICRF heating of both electrons and ions has been demonstrated at

modest ICRF power levels. Initial measurements of alpha ash suggest that helium transport in the plasma core will not be a fundamental limiting factor for helium exhaust in a reactor with supershot-like transport. The high power deuterium and tritium experiments on TFTR have provided the first look at the effect on MHD activity of a fusion α population similar to that expected on ITER. In the TFTR DT experiments to date there is no evidence for α loss due to α-driven instabilities; however, one of the highest fusion power shots may have evidence of α-driven TAE activity. Theoretical calculations suggest that presently achieved α parameters in TFTR are close to the stability threshold for α-driven TAE modes. The limiter H-modes in D-T plasmas have better confinement than those in D, but have larger ELMs. The presence of more virulent ELMs may increase the challenge of plasma-wall interactions and divertor problems on ITER.

Since the β-limit is now providing a fundamental limitation on the achievable DT performance in TFTR, the toroidal magnetic field was recently increased from 5.2 T to 5.6 T and a further increase to 6.0 T is planned for a limited number of pulses. This allows stable operation at high plasma current. Such an increase could raise the central plasma energy density at the β-limit by up to 30% and, if the present scaling is maintained, the achievable DT fusion power by up to 60%.

ACKNOWLEDGMENTS

The authors express their appreciation to the technical, engineering and scientific staff who enabled the execution of these important D-T experiments, to our collaborators on whose expertise we relied, and to Drs. R. C. Davidson and P. Rutherford for their support and encouragement.

Work supported by U. S. Department of Energy Contract No. DE-AC02-76-CH03073.

References

[1] D. E. Post, Plasma Physics and Controlled Nuclear Fusion Research (Proc. 13th Int. Conf., Washington, 1990) (International Atomic Energy Agency, Vienna 1991), Vol. 3, p. 239.

[2] R. J. Hawryluk, D. Mueller, J. Hosea, C. W. Barnes, M. Beer, M. G. Bell, R. Bell, H. Biglari, M. Bitter, R. Boivin, N. L. Bretz, R. Budny, C. E. Bush, L. Chen, C. Z. Cheng, S. C. Cowley, D. S. Darrow, P. C. Efthimion, R. J. Fonck, E. Fredrickson, H. P. Furth, G. Greene, B. Grek, L. R. Grisham, G. Hammett, W. Heidbrink, K. W. Hill, D. Hoffman, R. A. Hulse, H. Hsuan, A. Janos, D. L. Jassby, F. C. Jobes, D. W. Johnson, L. C. Johnson, J. Kamperschroer, J. Kesner, C. K. Phillips, S. J. Kilpatrick, H. Kugel, P.H. Lamarche, B. Leblanc, D.M. Manos, D.K. Mansfield, E. S. Marmar, E. Mazzucato, M. P. Mccarthy, J. Machuzak, M. Mauel, D. C. Mccune, K. M. McGuire, S. S. Medley, D. R. Mikkelsen, D. A. Monticello, Y. Nagayama, G. A. Navratil, R. Nazikian, D. K. Owens, H. Park, W. Park, S. Paul, F. W. Perkins, S. Pitcher, D. Rasmussen, M. H. Redi, G. Rewoldt, D. Roberts, A. L. Roquemore, S. Sabbagh, G. Schilling, J. Schivell, G. L. Schmidt, S. D. Scott, J. Snipes, J. Stevens, B. C. Stratton, J. D. Strachan, W. Stodiek, E. Synakowski, W. Tang, G. Taylor, J. Terry, J. R. Timberlake, H. H. Towner, M. Ulrickson, S. Von Goeler, R. M. Wieland, J. R. Wilson, K. L. Wong, P. Woskov, M. Yamada, K. M. Young, M. C. Zarnstorff, S. J. Zweben, Fusion Technology, **21**, 1324 (1992) .

[3] R. J. Hawryluk, H. Adler, P. Alling, C. Ancher, H. Anderson, J. L. Anderson, J. W. Anderson, V. Arunasalam, G. Ascione, D. Ashcroft, C. W. Barnes, G. Barnes, S. Batha, G. Bateman, M. Beer, M. G. Bell, R. Bell, M. Bitter, W. Blanchard, N. L. Bretz, C. Brunkhorst, R. Budny, C. E. Bush, R. Camp, M. Caorlin, H. Carnevale, S. Cauffman, Z. Chang, C.Z. Cheng, J. Chrzanowski, J. Collins, G. Coward,

M. Cropper, D. S. Darrow, R. Daugert, J. Delooper, W. Dorland, L. Dudek, H. Duong, R. Durst, P. C. Efthimion, D. Ernst, H. Evenson, N. J. Fisch, R. Fisher, R. J. Fonck, E. Fredd, E. Fredrickson, N. Fromm, G-Y. Fu, T. Fujita, H. P. Furth, V. Garzotto, C. Gentile, J. Gilbert, J. Gioia, N. Gorelenkov, B. Grek, L.R. Grisham, G. Hammett, G. R. Hanson, W. Heidbrink, H. W. Herrmann, K. W. Hill, J. Hosea, H. Hsuan, M. Hughes, R. Hulse, A. Janos, D. L. Jassby, F. C. Jobes, D. W. Johnson, L. C. Johnson, M. Kalish, J. Kamperschroer, J. Kesner, H. Kugel, G. Labik, N. T. Lam, P. H. Lamarche, E. Lawson, B. Leblanc, J. Levine, F. M. Levinton, D. Loesser, D. Long, M. J. Loughlin, J. Machuzak, R. Majeski, D. K. Mansfield, E. S. Marmar, R. Marsala, A. Martin, G. Martin, E. Mazzucato, M. Mauel, M. P. Mccarthy, J. Mcchesney, B. Mccormack, D. C. Mccune, K. M. McGuire, G. Mckee, D. M. Meade, S. S. Medley, D. R. Mikkelsen, S. V. Mirnov, D. Mueller, M. Murakami, J. A. Murphy, A. Nagy, G. A. Navratil, R. Nazikian, R. Newman, M. Norris, T. O'connor, M. Oldaker, J. Ongena, M. Osakabe, D. K. Owens, H. Park, W. Park, P. Parks, S. F. Paul, G. Pearson, E. Perry, R. Persing, M. Petrov, C. K. Phillips, M. Phillips, S. Pitcher, R. Pysher, A.L. Qualls, S. Raftopoulos, S. Ramakrishnan, A. Ramsey, D. A. Rasmussen, M. H. Redi, G. Renda, G. Rewoldt, D. Roberts, J. Rogers, R. Rossmassler, A. L. Roquemore, E. Ruskov, S. A. Sabbagh, M. Sasao, G. Schilling, J. Schivell, G. L. Schmidt, R. Scillia, S. D. Scott, I. Semenov, T. Senko, S. Sesnic, R. Sissingh, C. H. Skinner, J. Snipes, J. R. Stencel, J. Stevens, T. Stevenson, B. C. Stratton, J. D. Strachan, W. Stodiek, J. Swanson, E. Synakowski, H. Takahashi, W. M. Tang, G. Taylor, J. Terry, M. E. Thompson, W. Tighe, J. R. Timberlake, K. Tobita, H. H. Towner, M. Tuszewski, A. Von Halle, C. Vannoy, M. Viola, S. Von Goeler, D. Voorhees, R.T. Walters, R. Wester, R. B. White, R. Wieland, J. B. Wilgen, M. D. Williams, J. R. Wilson, J. Winston, K. Wright, K. L. Wong, P. Woskov G. A. Wurden, M. Yamada, S. Yoshikawa, K. M. Young, M. C. Zarnstorff, V. Zavereev, and S. J. Zweben, Plasma Physics and

Controlled Nuclear Fusion Research (Proc. 15th Int. Conf., Seville, 1994) (International Atomic Energy Agency, Vienna, 1995), IAEA-CN-60/A-2-II-5.

[4] The JET Team, Nuclear Fusion **32**, 187 (1992) .

[5] J. L. ANDERSON, R.A.P. SISSINGH, C.A. GENTILE, R.L. ROSSMASSLER, R.T. WALTERS, D.R. VOORHEES, Proc. 15th IEEE/NPSS Symposium on Fusion Engineering, Hyannis, October 1993, *to be published* .

[6] J. D. Strachan, 21st European Physical Society Meeting of the Plasma Physics Division (Montpellier, France, June 27-July 1, 1994).

[7] G. A. Wurden, R. E. Chrien, C. W. Barnes, "A Scintillating Fiber 14-MeV Neutron Detector on TFTR During DT Operation", accepted for publication in Rev. Sci. Instrum. 66(1), January, 1995.

[8] J. D. Strachan, Phys. Rev. Lett. **72**, 3526 (1994), and references therein.

[9] R. Hawryluk, Phys. Rev. Lett. **72**, 3530 (1994).

[10] J. D. Strachan, Phys. Rev. Lett. **72**, 3526 (1994).

[10a] P. C. Efthimion, Plasma Physics and Controlled Nuclear Fusion Research (Proc. 15th Int. Conf., Seville, 1994) (International Atomic Energy Agency, Vienna, 1995), IAEA-CN-60/A-2-II-6 and references therein.

[11] E. J. Synakowski, Phys. Fluids B **5**, 2215 (1993).

[12] E. J. Synakowski, Phys. Rev. Lett. **65**, 2255 (1990).

[13] P. C. Efthimion, Phys. Rev. Lett. **66**, 421 (1991).

[14] R. V. BUDNY, Proceedings of the 21st European Physical Society Meeting of the Plasma Physics Division, (Montpellier, France, June 27-July 1, 1994).

[15] M. C. Zarnstorff, Plasma Physics and Controlled Nuclear Fusion Research (Proc. 15th Int. Conf., Seville, 1994) (International Atomic Energy Agency, Vienna, 1995), IAEA-CN-60/A-2-I-2 and references therein.

[16] S. A. Sabbagh, Plasma Physics and Controlled Nuclear Fusion Research (Proc. 15th Int. Conf., Seville, 1994) (International Atomic Energy Agency, Vienna, 1995), IAEA-CN-60/A-5-I-6 and references therein.

[17] C. E. Bush, S. A. Sabbagh, R. E. Bell, E. J. Synakowski, M. Bell, S. Batha, R. Budny, N. L. Bretz, Z. Chang, D. S. Darrow, P. C. Efthimion, D. Ernst, E. Fredrickson, J. Kesner, F. M. Levinton, M. E. Mauel, G. A. Navratil, C. K. Phillips, S. D. Scott, G. Taylor, M. C. Zarnstorff, S. Zweben, Proc. 21th Eps Conference On Controlled Fusion And Plasma Physics, 1994.

[18] C. E. Bush, Proc. of the Annual Meeting of the American Physical Society Division of Plamsa Physics, Minneapolis, November 1994.

[19] S. J. Zweben, Phys. Plasmas **1** (5), 1469 (1994).

[20] D. S. DARROW, S. J. ZWEBEN, R. V. BUDNY, Princeton Plasma Physics Report PPPL-2975, Oct. 1994.

[21] Z. Y. Chang, Nucl. Fusion, accepted for publication, (1994).

[22] S. Zweben, Phys. of Plasmas **1**, 1469 (1994).

[23] F. Troyon, A. Roy, W. A. Cooper, F. Yasseen, and A. Turnbull, Plasma Phys. Controlled Fusion **30**, 1597 (1988).

[24] E. Fredrickson, K. M. McGuire, Princeton Plasma Physics Report PPPL-3023, Sept. 1994, (submitted to Phys. of Plasmas).

[25] R. C. Grimm, J. M. Greene, J. L. Johnson, Computational Physics **16**, 253 (1976) .

[26] F. Levinton, L. Zakharov, S. H. Batha, J. Manickam, M. C. Zarnstorff, Phys. Rev. Lett. **72**, 2895 (1994).

[27] R. J. Hastie, JET LABORATORY REPORT, JET-R(94)03, MAY 1994.

[28] K. L. Wong, R. J. Fonck S. P. Paul, Phys. Rev. Lett. **66**, 1874 (1994).

[29] W. W. Heidbrink, E. J. Strait, E. Doyle, G. Sager, And R. T. Snider, Nucl. Fusion **31**, 1635 (1991).

[30] C. Z. Cheng, Plasma Physics and Controlled Nuclear Fusion Research (Proc. 15th Int. Conf., Seville, 1994) (International Atomic Energy Agency, Vienna, 1995), IAEA-CN-60/D-3-III-2.

[31] D. Spong, Plasma Physics and Controlled Nuclear Fusion Research (Proc. 15th Int. Conf., Seville, 1994) (International Atomic Energy Agency, Vienna, 1995), IAEA-CN-60/D-P-II-3.

[32] E. Fredrickson, S. Batha, M. Bell, R. Budny, C. Bush, Z. Chang, C. Z. Cheng, D. S. Darrow, J. Dunlap, G.Y. Fu, H. W. Herrmann, H. Hsuan, R. Majeski, D. K. Mansfield, E. Mazzucato, K. M. McGuire, D. R. Mikkelsen, M. Murakami, R. Nazikian, A. Janos, C. K. Phillips, S. A. Sabbagh, G. L. Schmidt, S. D. Scott, J. D. Strachan, E. Synakowski, H. Takahashi, G. Taylor, J. R. Wilson, K. L. Wong, M. C. Zarnstorff, S. Zweben, Plasma Physics and Controlled Nuclear Fusion Research (Proc. 15th Int. Conf., Seville, 1994) (International Atomic Energy Agency, Vienna, 1995), IAEA-CN-60/A-2-II-5.

[33] C. Z. Cheng, Physics Reports **2111**, 1 (1992).

[34] G. Y. Fu, C. Z. Cheng, K. L. Wong, Phys. Fluids B**5**, 4040 (1993).

[35] R. Majeski, N. J. Fisch, H. Adler, S. Batha, M. G. Bell, R. Bell, M. Bitter, N. I. Bretz, R. Budny, C. E. Bush, S. Cauffman, Z. Chang, D. Darrow, A. C. England, E.

Fredrickson, H. P. Furth, B. Grek, G. R. Hanson, M. C. Herrman, K. Hill, J. C. Hosea, H. Hsuan, D. Ignat, E. F. Jaeger, A. C. Janos, F. C. Jobes, D. W. Johnson, L. C. Johnson, C. F. F. Karney, B. Leblanc, F. Levinton, E. Mazzucato, S. S. Medley, D. Mikkelsen, D. Mueller, M. Murakami, H. E. Mynick, R. Nazikian, D. K. Owens, H. Park, C. K. Phillips, A. T. Ramsey, D. A. Rasmussen,2 J. M. Rax, J. H. Rogers, G. Schilling, J. Schivell, S. D. Scott, P. Snyder, J. E. Stevens, E. Synakowski, G. Taylor, E. J. Valeo, Z. H. Wang, J. B. Wilgen, J. R. Wilson, K. L. Wong, M. C. Zarnstorff, and S. J. Zweben, Plasma Physics and Controlled Nuclear Fusion Research (Proc. 15th Int. Conference, Seville, 1994) (International Atomic Energy Agency, Vienna, 1995), IAEA-CN-60/A-3-I-4.

[36] R. Majeski, D. K. Phillips, J. R. Wilson, Phys. Rev. Lett. **73**, 2204 (1994).

[37] D. Spong, Plasma Physics and Controlled Nuclear Fusion Research (Proc. 15th Int. Conf., Seville, 1994) (International Atomic Energy Agency, Vienna, 1995), IAEA-CN-60/D-P-II-3.

[38] F. Zonca, L. Chen, Phys Fluids B **5**, 3668 (1993).

[39] J. F. Clarke, Nucl. Fusion **20**, 563 (1980).

[40] N. Fisch, J.-M. Rax, Plasma Physics and Controlled Nuclear Fusion Research (Proc. 14th. Int. Conf., Würzburg, 1992) (International Atomic Energy Agency, Vienna, 1993), Vol. 1, p. 769.

Figure Captions

Fig. 1 Progress of tokamaks in obtaining fusion power from DD and DT reactions for OH, NBI, and RF heated plasmas.

Fig. 2. Peak D-T fusion power for TFTR discharges in the supershot, high-βp, and L-mode regimes.

Fig. 3. Time evolution of the DT fusion power from a sequence in December 1993 and May 1994, leading up to the shot producing the highest instantaneous power of 9.3 MW at 32 MW of input power for an instantaneous Q of 0.27.

Fig. 4. Measured profiles of neutron emission compared with those calculated by TRANSP fro measured plasma parameters.

Fig. 5. Comparison of tritium and helium particle diffusivities and convective velocities. The diffusivities of tritium, helium, and heat are of similar magnitudes. These are attractive characteristics for future reactors, like ITER.

Fig. 6. Comparison of plasma stored energy in comparable DD and DT discharges. The plasma stored energy is larger in the DT plasmas. Energy confinement time increases from 160 ms to 200 ms. The product $n_i(0)T_i(0)\tau_E$ increases from 1.9 to 3.5 ($10^{20}m^{-3}$•s•keV).

Fig. 7. The energy confinement time in these supershot discharges increased with the average mass of the hydrogenic ions. This is observed in supershot and H-mode regimes.

Fig. 8. Ion temperature and electron density profiles for an Ip = 1.6 MA plasma with 8 MA of tritium and 8 MW of deuterium NBI. There is a 20-30% increase in Ti(0) and a 5-10% increase in the ne(0) going from DD to DT plasmas.

Fig. 9 Ion thermal conductivity is reduced by a factor of ≈2 in DT plasma compared to DD plasmas. The improvement in χ_i increases with plasma tritium content.

Fig. 10 Comparison of H-mode transitions in DD and DT plasmas. The increase in τ_E is larger in DT plasmas. The edge localized modes are larger in DT plasmas.

Fig. 11. Initial results fro BES indicate that there appears to be a reduction in the local ñ/n in DT plasmas compared to similar DD cases.

Fig. 12 The plasma current dependence of the neutron-normalized total D-T alpha loss signals. The agreement between the calculated and measured alpha loss versus plasma current is within the estimated uncertainties in the calculation.

Fig. 13 (a) Neutron-normalized alpha loss rate to a detector 90∞ below the midplane as a function of time and (b) the corresponding RF power evolution. 9.1 MW of D and 11.6 MW of T neutral beam power were injected during the time indicated by the shaded region.

Fig. 14 Energy spectrum of confined alpha particles measured by the alpha charge exchange diagnostic at r=18 cm is compared with TRANSP calculation.

Fig. 15 The effects of MHD on confinement suggests that the MHD can be responsible for up to a 30% decrease in the energy confinement time in the worst cases. In cases of weak MHD, typical of most of the higher current plasma (Ip>2 MA, qsh<4), the effect is usually less than 5%.

Fig. 16 Contours of the electron temperature prior to a high b disruption showing the n=1 kink and ballooning precursors.

Fig. 17 Alpha loss does not increase with fusion power on TFTR during DT. The variation of lost alpha fraction with fusion power is consistent with the first-orbit loss model.

Fig. 18 Spectrum of magnetic fluctuation for DT plasmas generating 7.5 MW and 6.2 MW of fusion power and a D-only plasma.

Fig. 19 Comparison of (a) ion and (b) electron temperature profiles for two DT plasmas. The discharge indicated by the bold solid line had 5.5 MW of ICRF heating.

Fig. 20 Measured power fraction to ions and electrons ($P_e + P_i$) and to electrons only (P_e) are shown by the solid lines plotted against tritium beam power fraction. Data is compared to RF code calculations shown by the dashed lines.

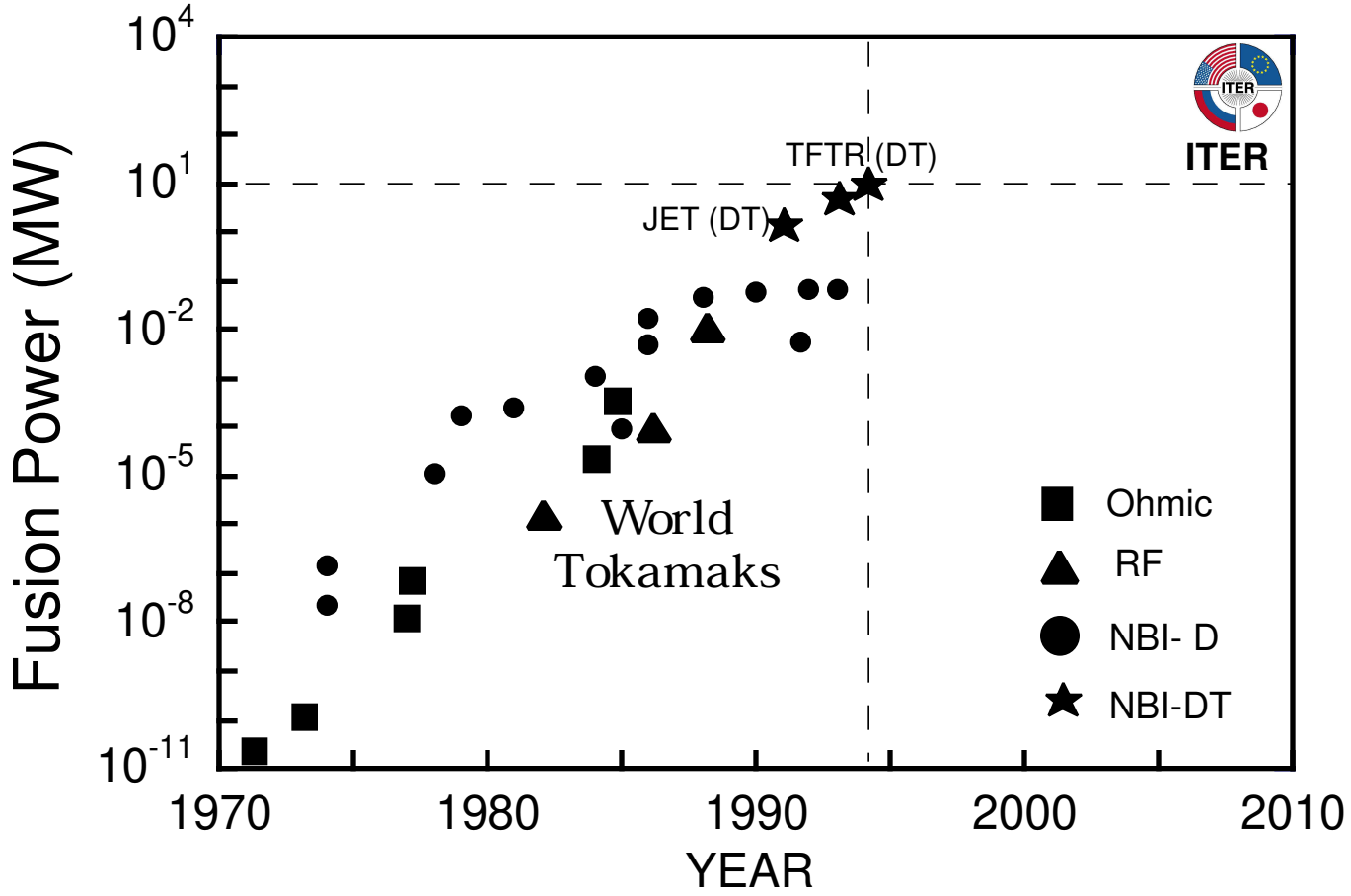
Fusion Power (MW)
10^{4}
10^{1}
10^{-2}
10^{-5}
10^{-8}
10^{-11}
1970
1980
1990
2000
2010
YEAR
TFTR (DT)
JET (DT)
ITER
World
Tokamaks
Ohmic
RF
NBI- D
NBI-DT

Figure 1

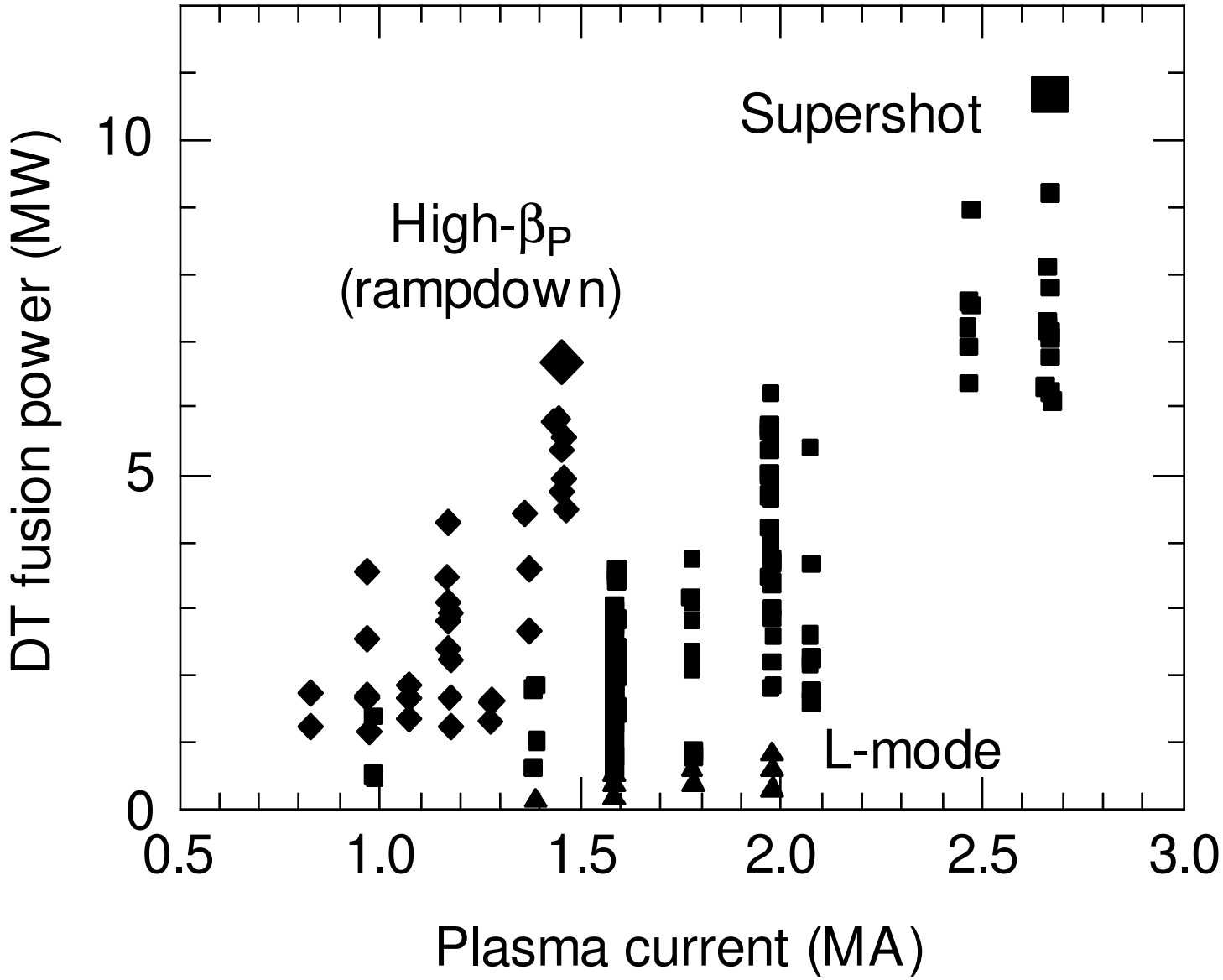
Supershot
High-β_P
(rampdown)
L-mode
DT fusion power (MW)
Plasma current (MA)
0
5
10
0.5
1.0
1.5
2.0
2.5
3.0

Figure 2

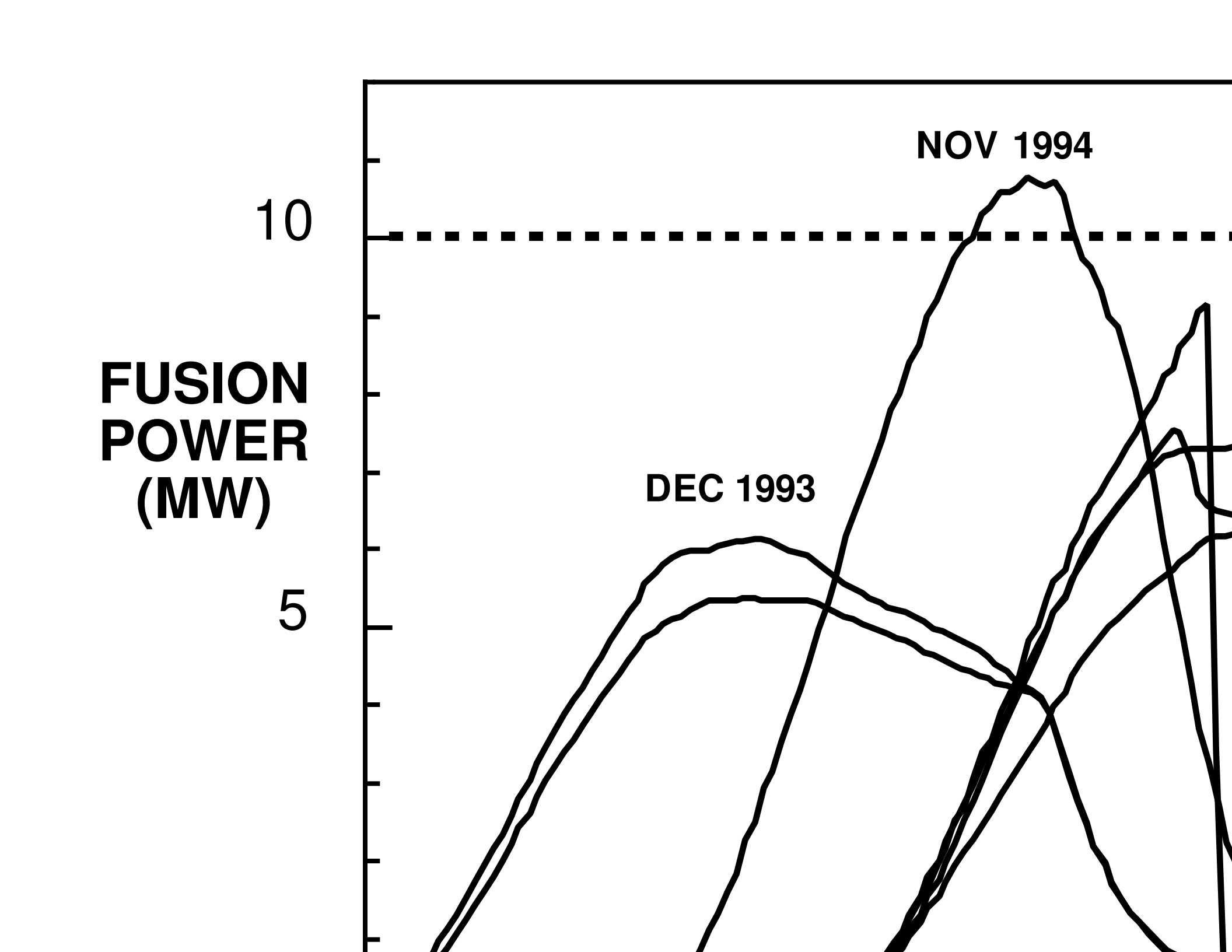
NOV 1994
DEC 1993
10
5
FUSION
POWER
(MW)

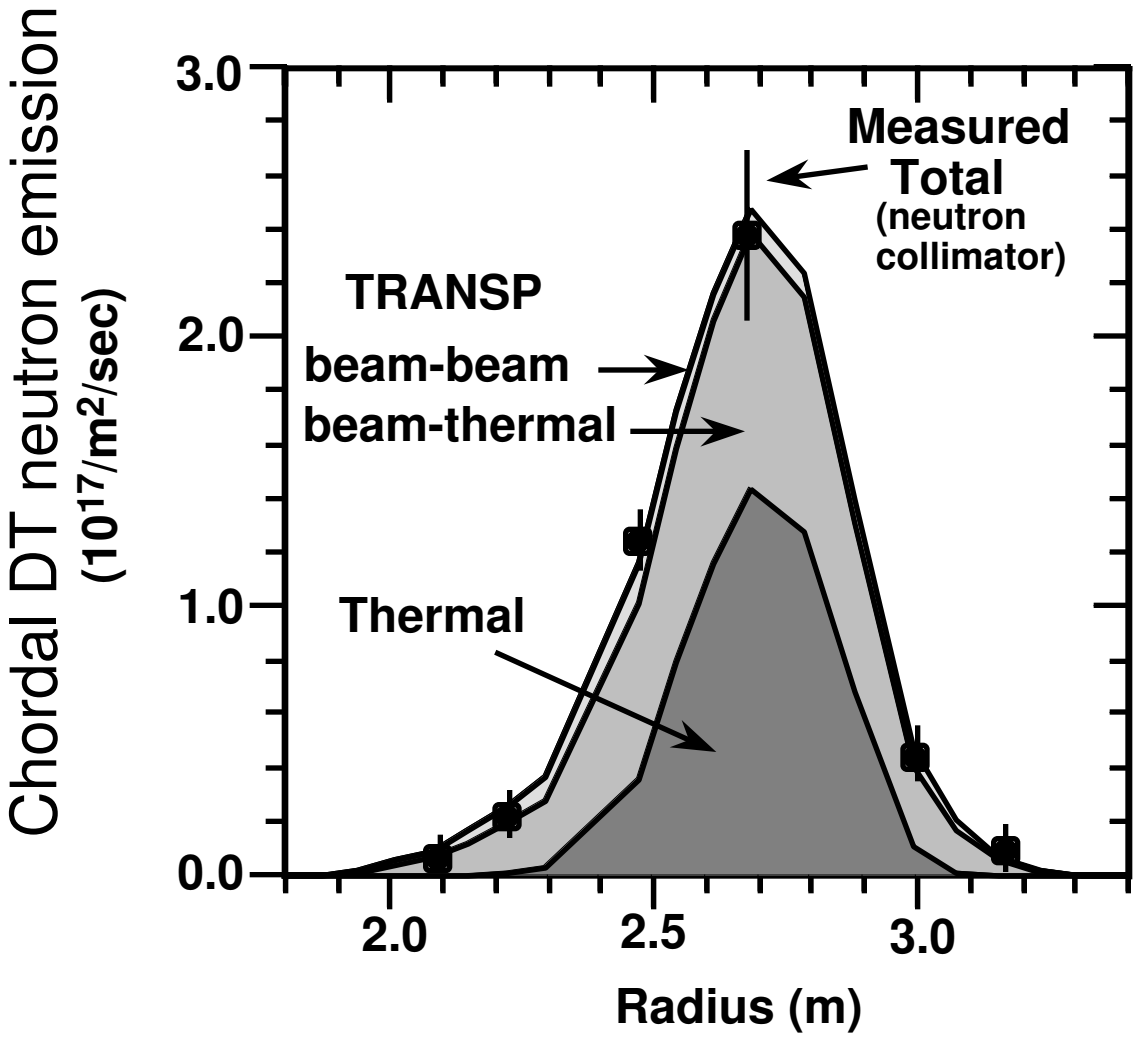
Chordal DT neutron emission
(10^17/m^2/sec)
3.0
2.0
1.0
0.0
2.0
2.5
3.0
Radius (m)
Measured
Total
(neutron
collimator)
TRANSP
beam-beam
beam-thermal
Thermal

Figure 4

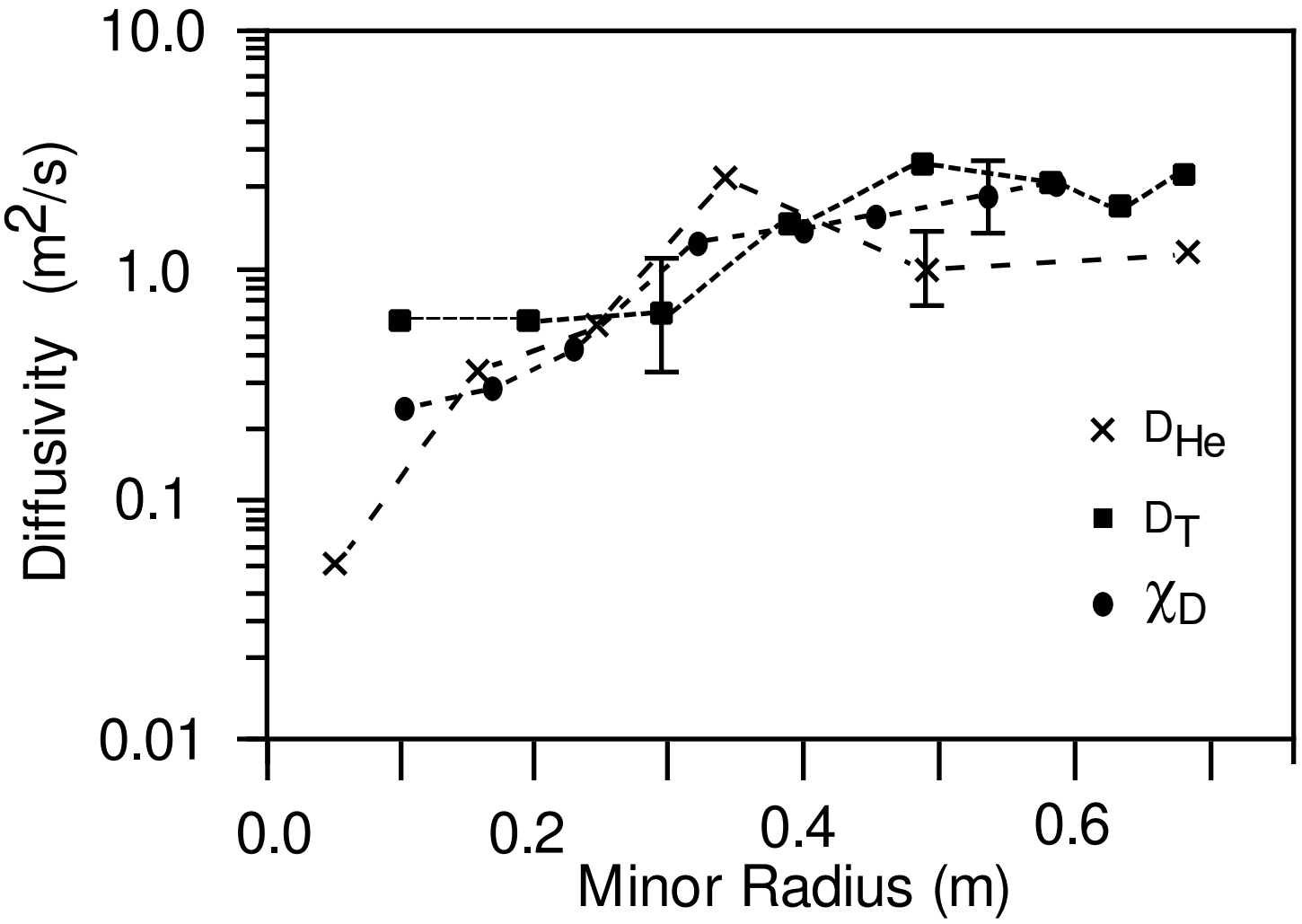
10.0
1.0
0.1
0.01
Diffusivity (m2/s)
0.0
0.2
0.4
0.6
Minor Radius (m)
DHe
DT
χD

Figure 5

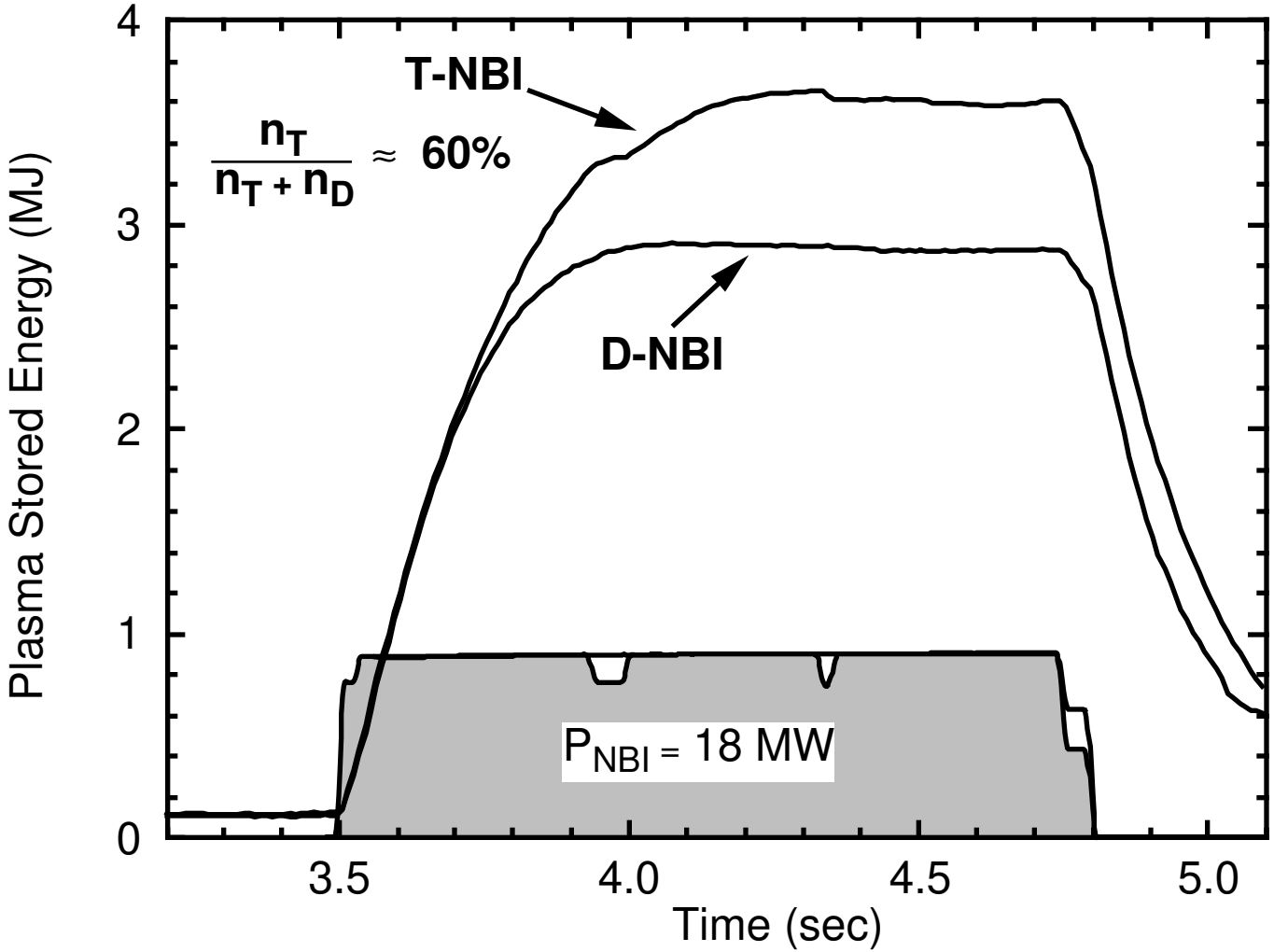
Plasma Stored Energy (MJ)
4
3
2
1
0
3.5
4.0
4.5
5.0
Time (sec)
T-NBI
D-NBI
$\frac{n_T}{n_T + n_D} \approx 60\%$
P_{NBI} = 18 MW

Figure 6

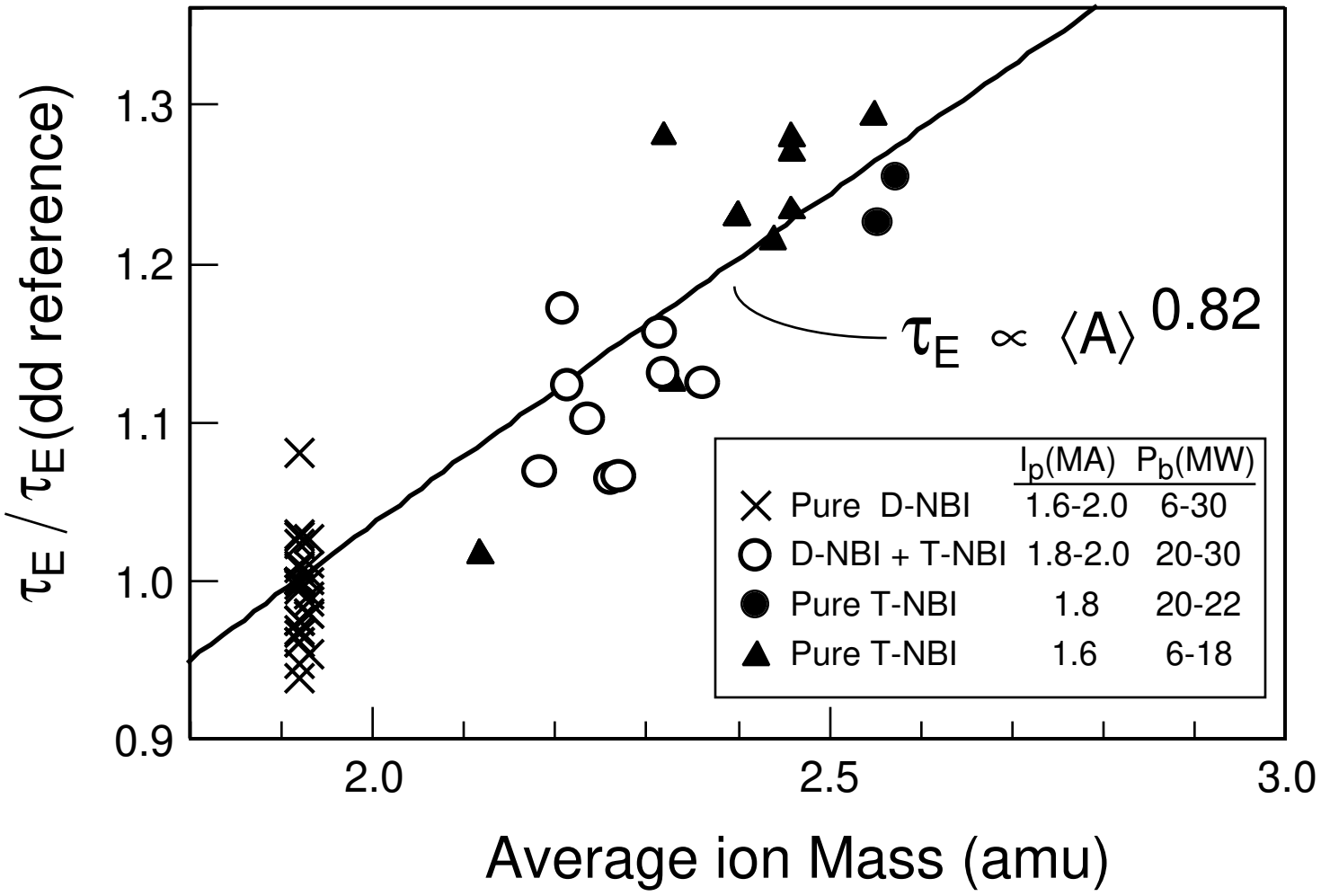
τ_E / τ_E(dd reference)
1.3
1.2
1.1
1.0
0.9
2.0
2.5
3.0
Average ion Mass (amu)
$\tau_E \propto \langle A \rangle^{0.82}$
I_p(MA) P_b(MW)
Pure D-NBI 1.6-2.0 6-30
D-NBI + T-NBI 1.8-2.0 20-30
Pure T-NBI 1.8 20-22
Pure T-NBI 1.6 6-18

Figure 7

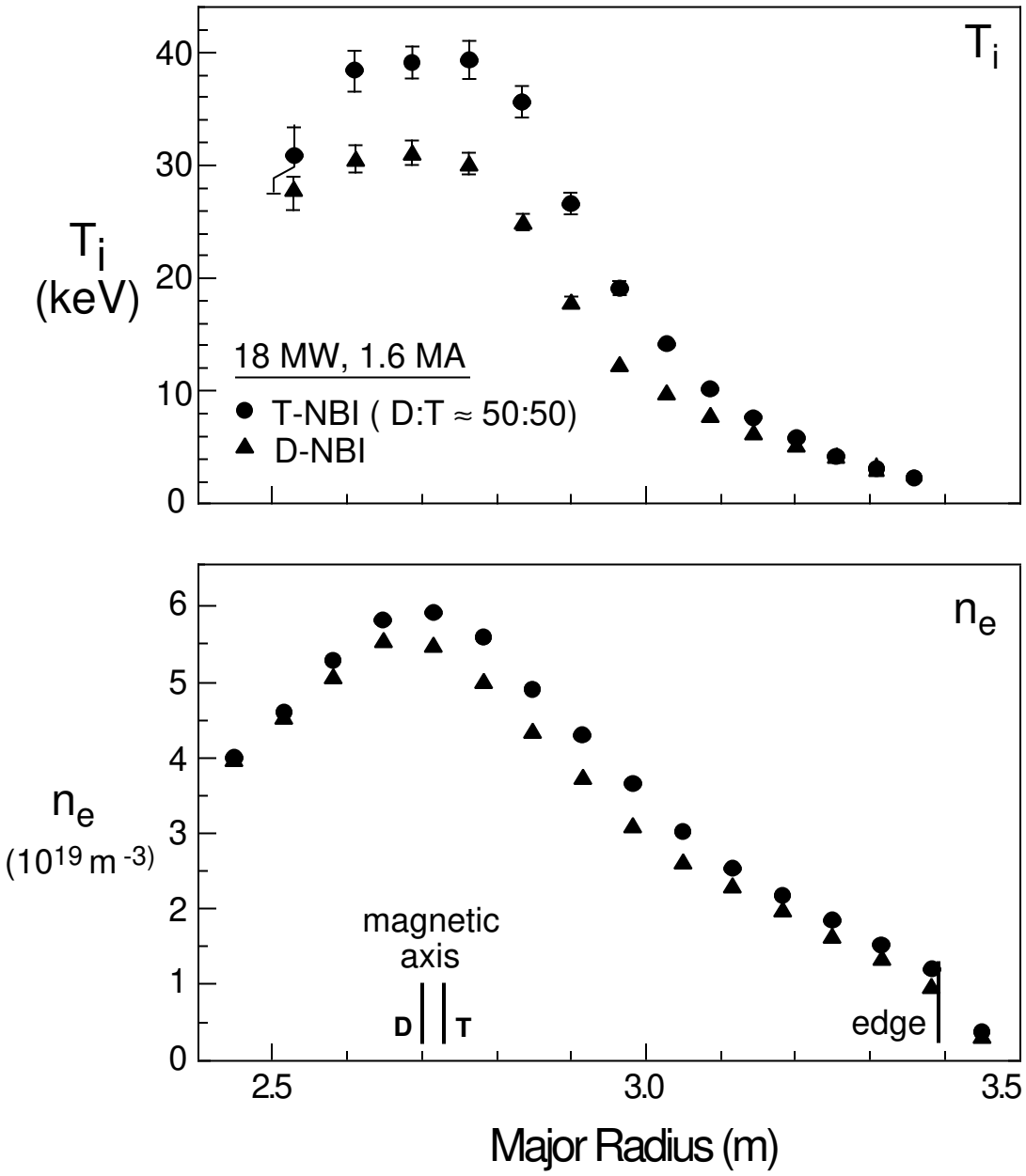
T_i
(keV)
40
30
20
10
0
T_i
18 MW, 1.6 MA
T-NBI (D:T ≈ 50:50)
D-NBI
n_e
$(10^{19}\,m^{-3})$
6
5
4
3
2
1
0
n_e
magnetic
axis
D
T
edge
2.5
3.0
3.5
Major Radius (m)

Figure 8

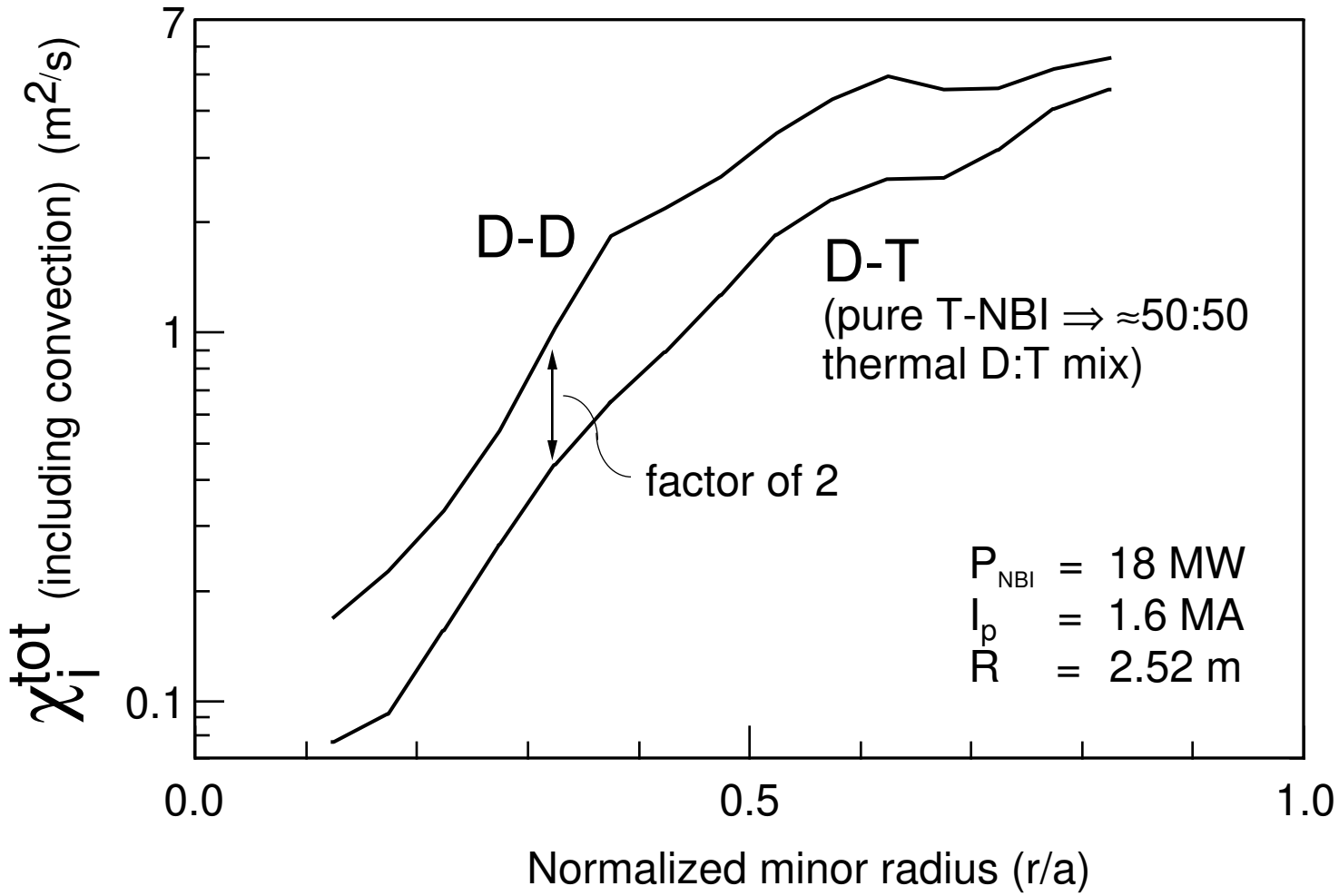
7
1
0.1
χ_i^{tot} (including convection) (m^2/s)
D-D
D-T
(pure T-NBI ⇒ ≈50:50
thermal D:T mix)
factor of 2
P_{NBI} = 18 MW
I_p = 1.6 MA
R = 2.52 m
0.0
0.5
1.0
Normalized minor radius (r/a)

Figure 9

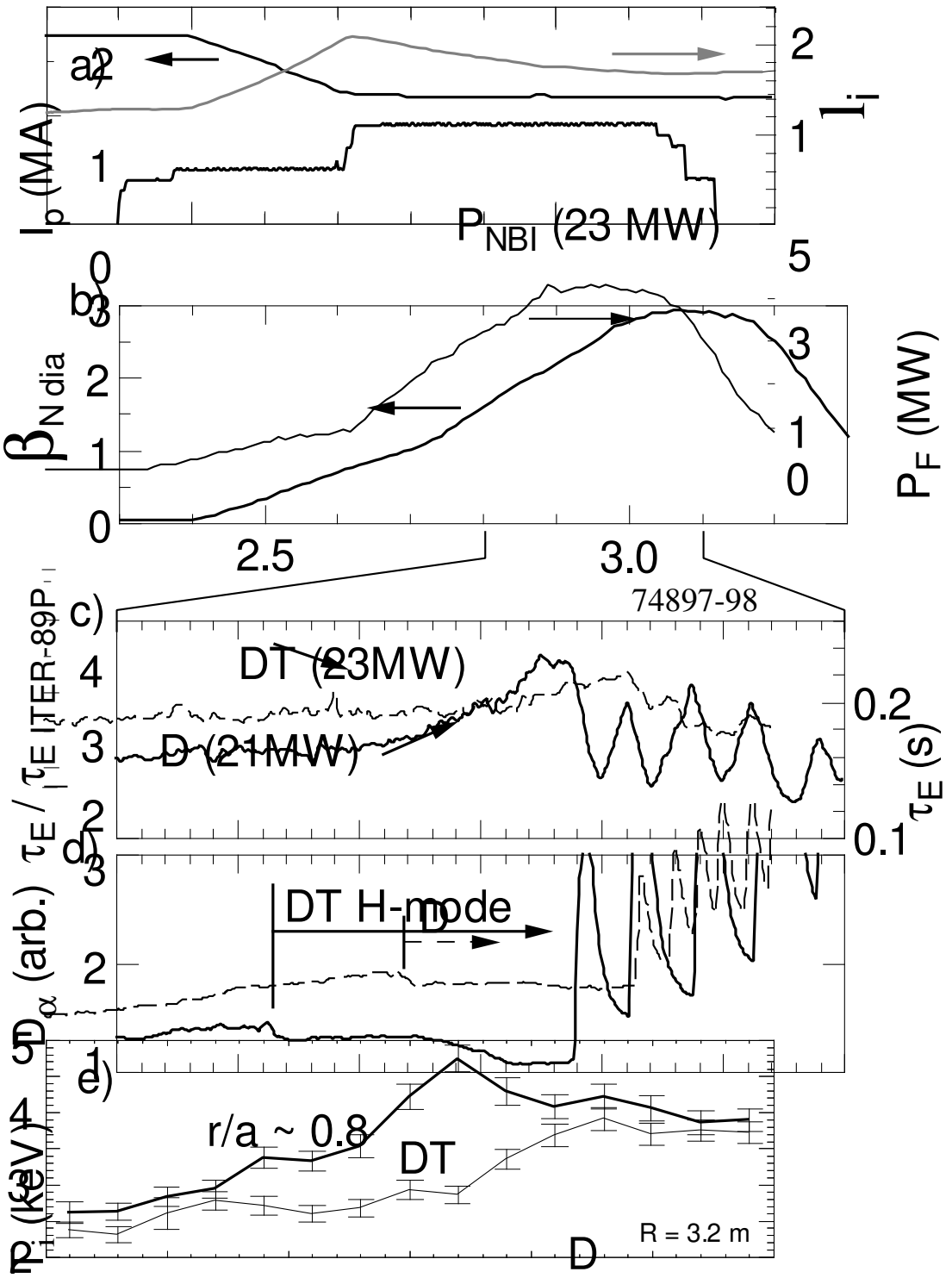
a)
I_p (MA)
l_i
P_{NBI} (23 MW)
b)
$\beta_{N\,dia}$
P_F (MW)
2.5
3.0
74897-98
c)
DT (23MW)
D (21MW)
$\tau_E / \tau_{E\,ITER-89P}$
τ_E (s)
d)
DT H-mode
D
D_α (arb.)
e)
r/a ~ 0.8
DT
R = 3.2 m
D
T_i (keV)
2.8
2.9
3.0
3.1
Time (sec)

Figure 10

There is no figure 11

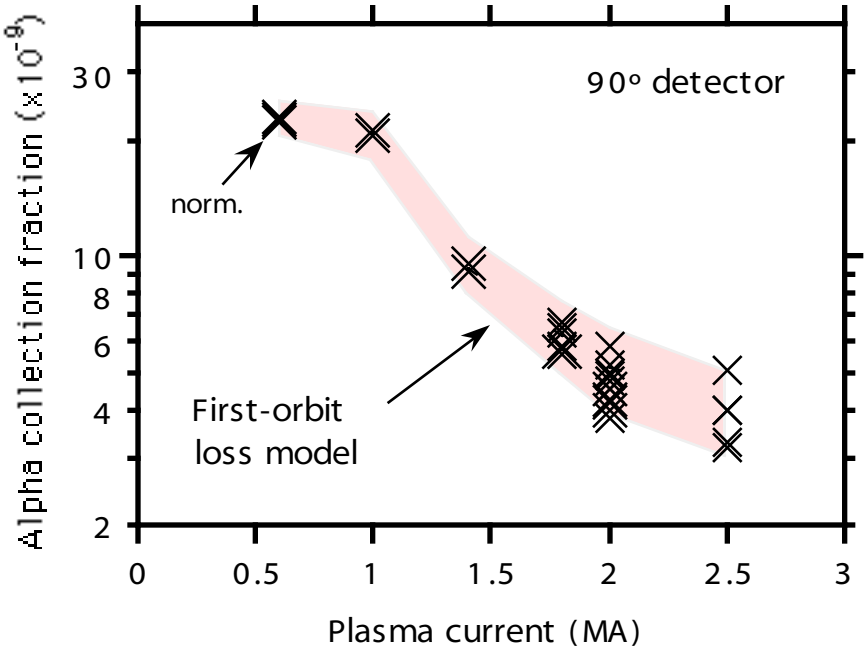
Alpha collection fraction (x10^{-9})
30
10
8
6
4
2
0
0.5
1
1.5
2
2.5
3
Plasma current (MA)
90° detector
norm.
First-orbit
loss model

Figure 12

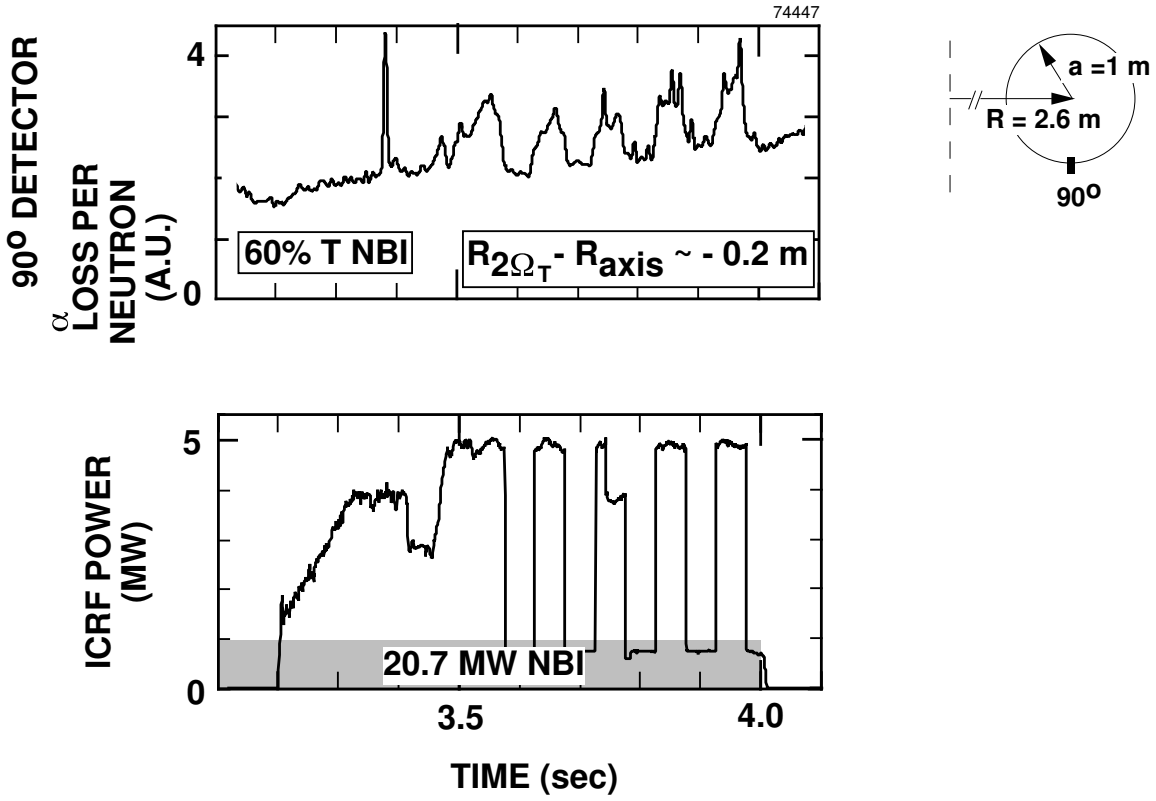
74447
90° DETECTOR
α LOSS PER NEUTRON (A.U.)
4
0
60% T NBI
$R_{2\Omega_T}$ - R_{axis} ~ - 0.2 m
a =1 m
R = 2.6 m
90°
ICRF POWER (MW)
5
0
20.7 MW NBI
3.5
4.0
TIME (sec)

Figure 13

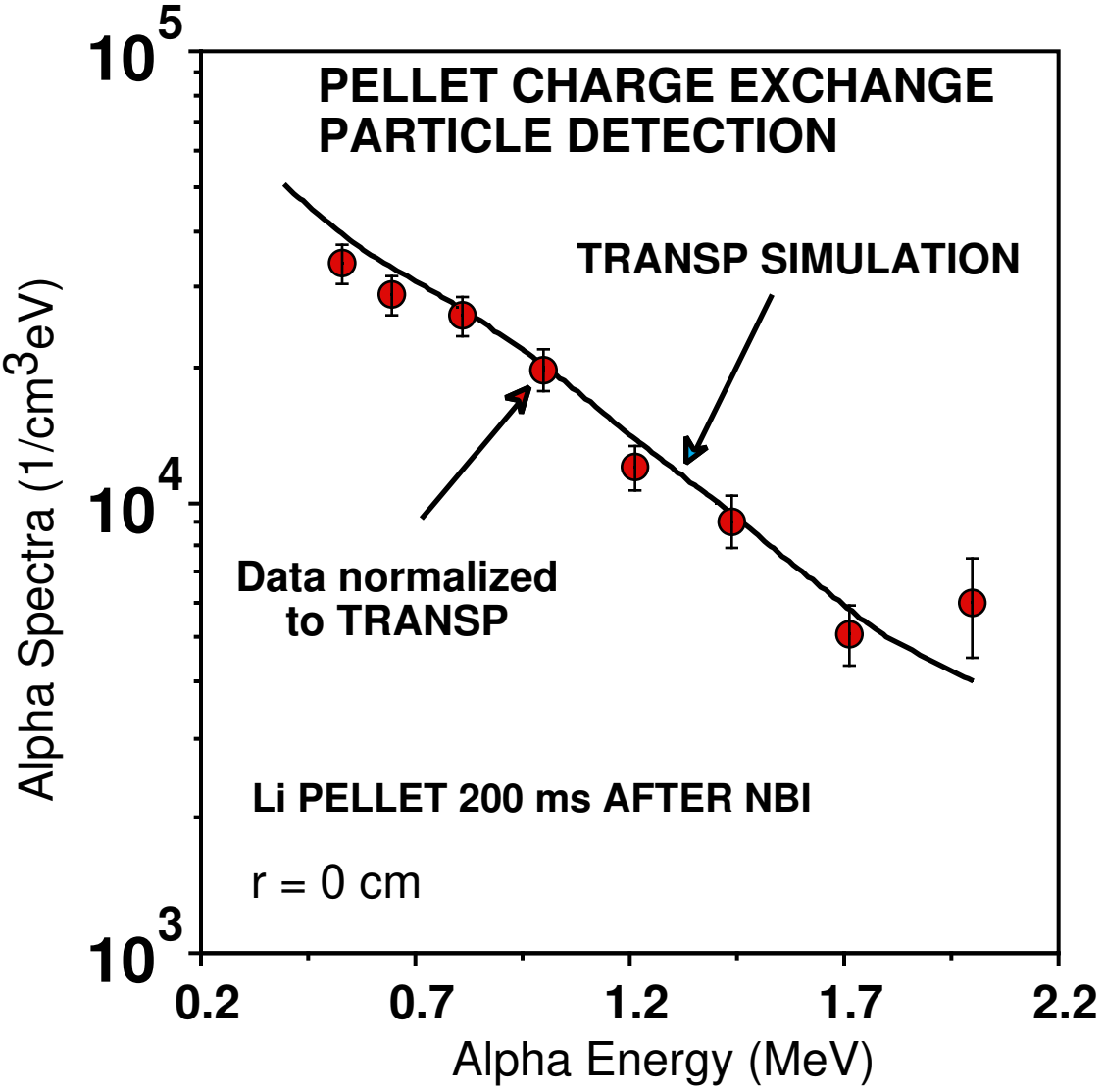
PELLET CHARGE EXCHANGE
PARTICLE DETECTION
TRANSP SIMULATION
Data normalized
to TRANSP
Li PELLET 200 ms AFTER NBI
r = 0 cm
Alpha Spectra (1/cm3eV)
Alpha Energy (MeV)
10^5
10^4
10^3
0.2
0.7
1.2
1.7
2.2

Figure 14

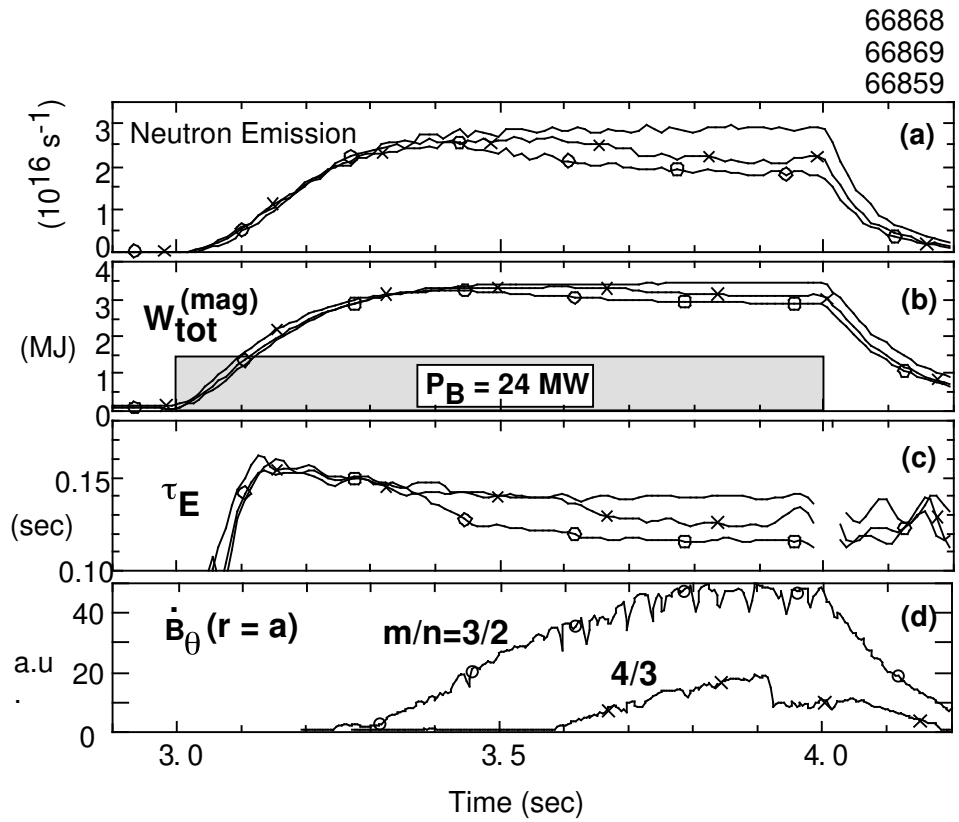
66868
66869
66859
Neutron Emission
(a)
(10^16 s^-1)
W_tot^(mag)
(b)
(MJ)
P_B = 24 MW
τ_E
(c)
(sec)
Ḃ_θ (r = a)
m/n=3/2
4/3
(d)
a.u.
3.0
3.5
4.0
Time (sec)

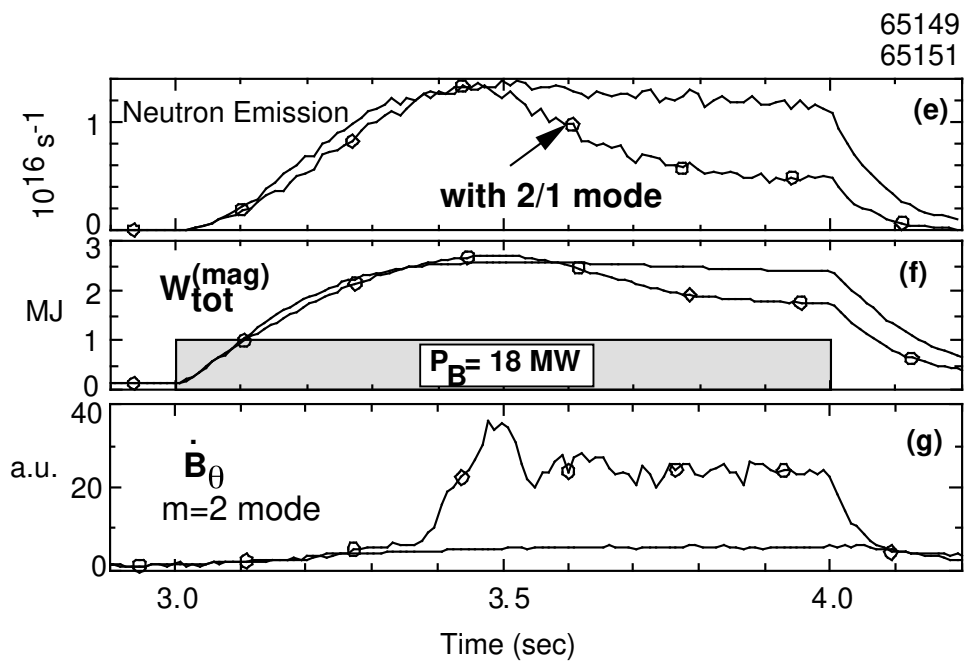
65149
65151
Neutron Emission
(e)
10^16 s^-1
with 2/1 mode
W_tot^(mag)
(f)
MJ
P_B= 18 MW
Ḃ_θ
m=2 mode
(g)
a.u.
3.0
3.5
4.0
Time (sec)

Figure 15

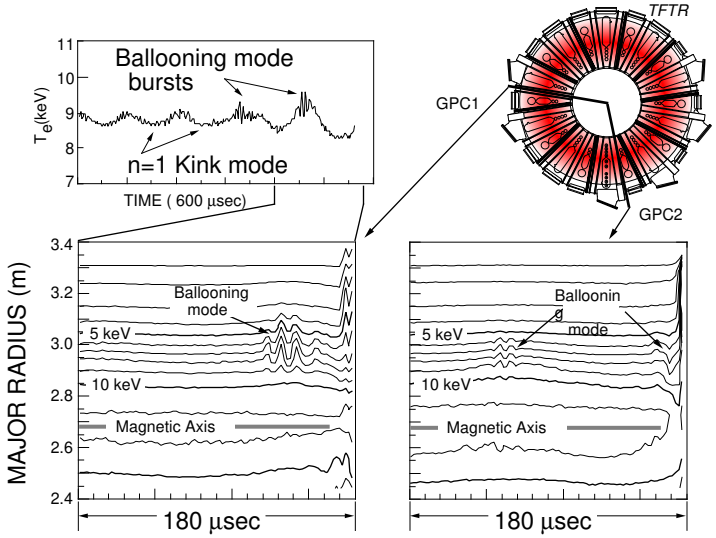
TFTR
GPC1
GPC2
Ballooning mode bursts
n=1 Kink mode
T_e(keV)
TIME (600 μsec)
MAJOR RADIUS (m)
Ballooning mode
5 keV
10 keV
Magnetic Axis
Balloonin g mode
180 μsec
180 μsec

Figure 16

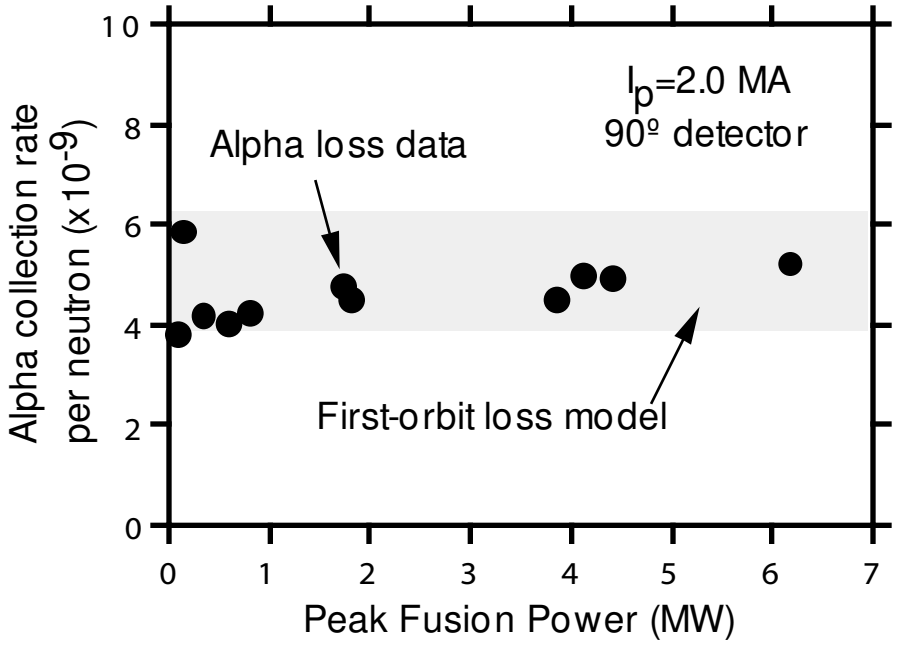
Alpha collection rate per neutron (x10-9)
10
8
6
4
2
0
0
1
2
3
4
5
6
7
Peak Fusion Power (MW)
Ip=2.0 MA
90º detector
Alpha loss data
First-orbit loss model

Figure 17

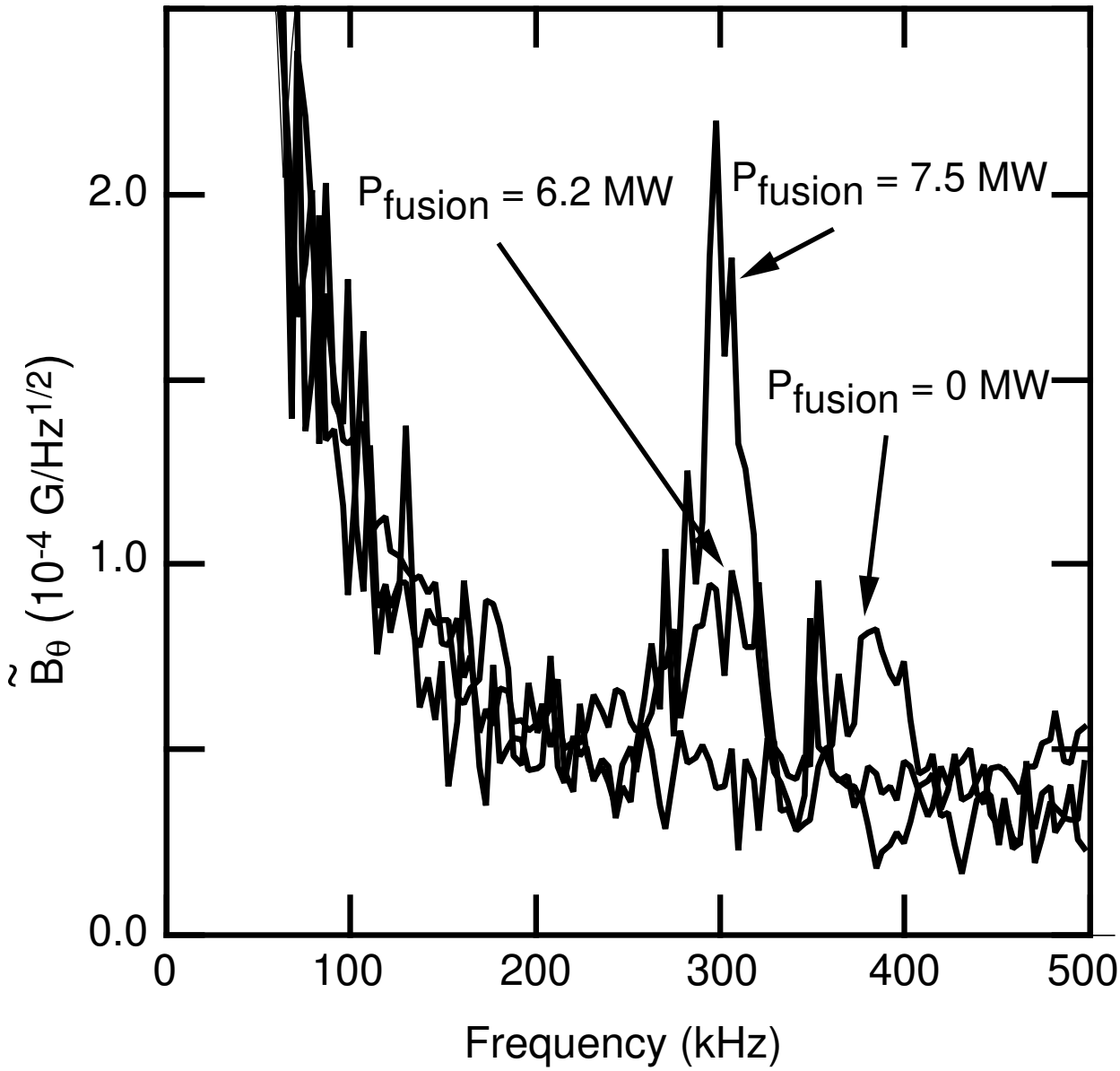
P_{fusion} = 6.2 MW
P_{fusion} = 7.5 MW
P_{fusion} = 0 MW
$\tilde{B}_\theta$ (10^{-4} G/Hz$^{1/2}$)
2.0
1.0
0.0
0
100
200
300
400
500
Frequency (kHz)

Figure 18

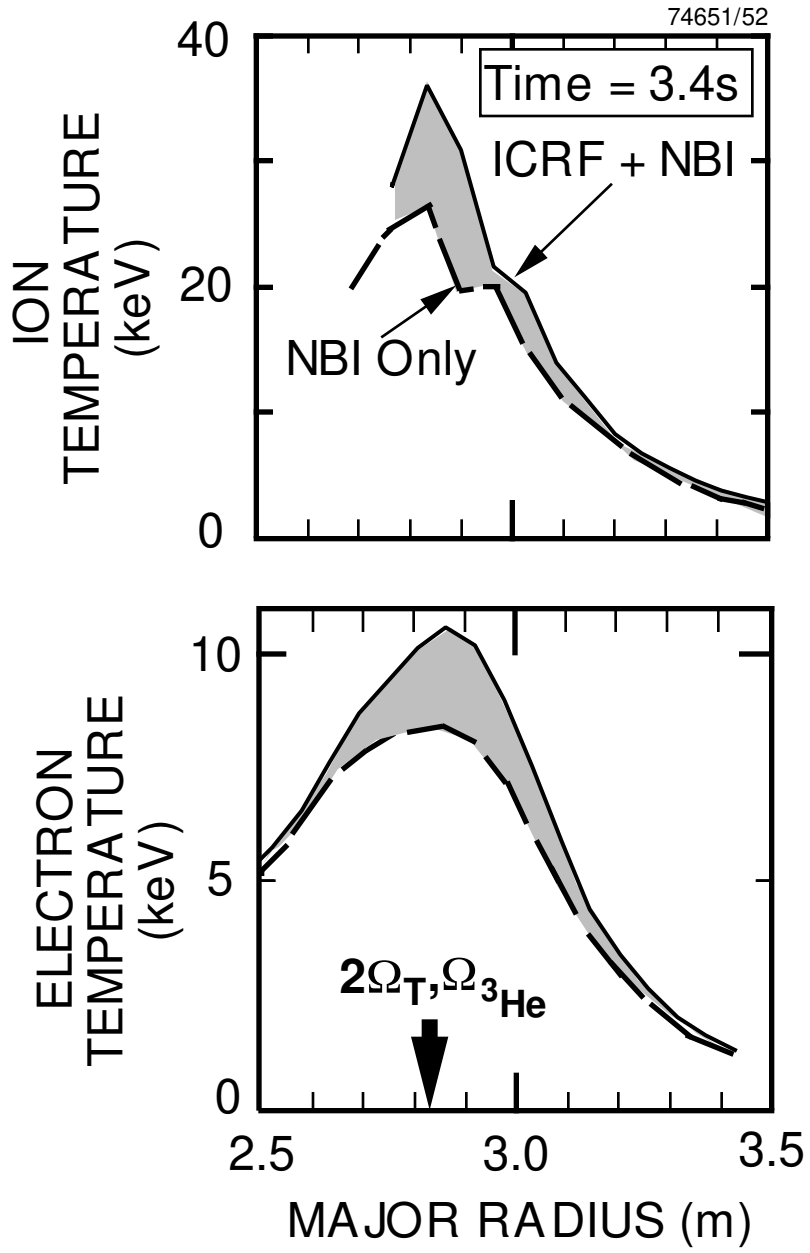
74651/52
40
20
0
ION TEMPERATURE (keV)
Time = 3.4s
ICRF + NBI
NBI Only
10
5
0
ELECTRON TEMPERATURE (keV)
$2\Omega_T, \Omega_{^3He}$
2.5
3.0
3.5
MAJOR RADIUS (m)

Figure 19

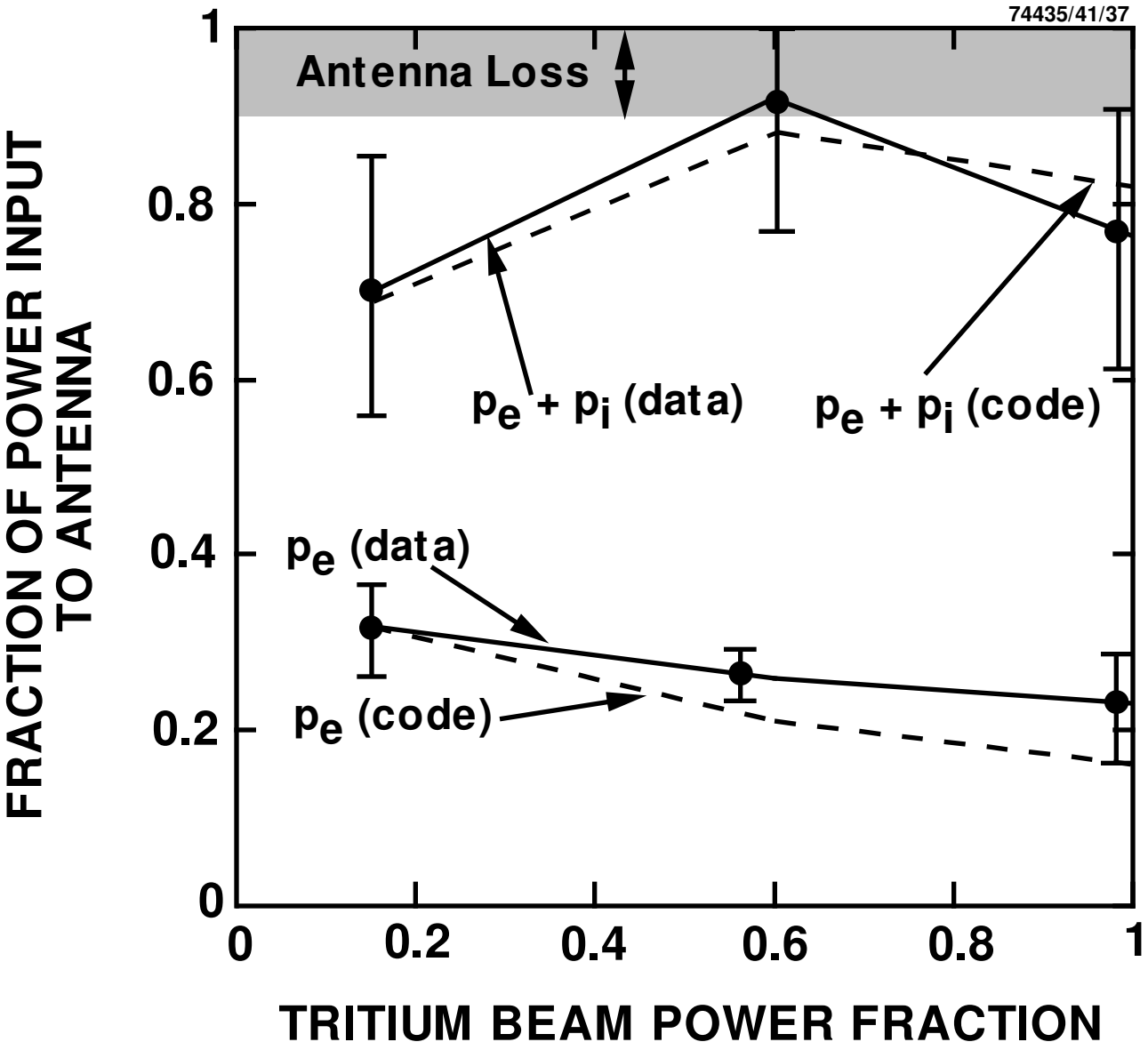
74435/41/37
Antenna Loss
$p_e + p_i$ (data)
$p_e + p_i$ (code)
p_e (data)
p_e (code)
FRACTION OF POWER INPUT TO ANTENNA
TRITIUM BEAM POWER FRACTION
0
0.2
0.4
0.6
0.8
1

FIgure 20

Confinement time can be increased with lithium conditioning

TFTR

- TFTR switched from confinement limited to stability limited.
- At the highest I_p and B, TFTR disrupted at less than maximum P_B and τ_E.
- Li pellet conditioning plus the DT isotope effect has tripled τ_E over L-mode.

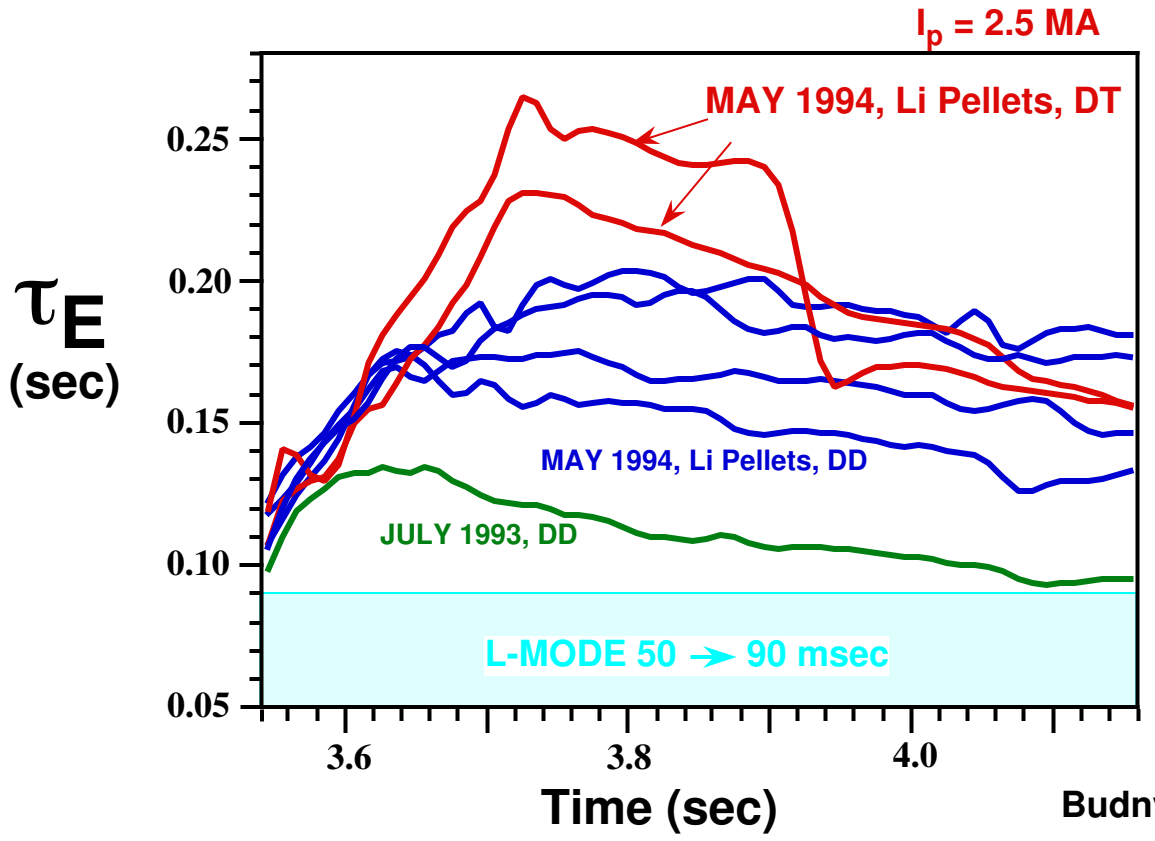

Budny 6Q 32

McG 94028

Comparison of Tritium and Helium Transport on TFTR

- Tritium density profile inferred from neutron emissivity. *TFTR*
- Transport coefficients (D_T, V_T) measured:
  $D_T \approx D_{He} \approx \chi_D$; $D_{He}/\chi_D \approx 1$
- Consistent with ExB drift theory

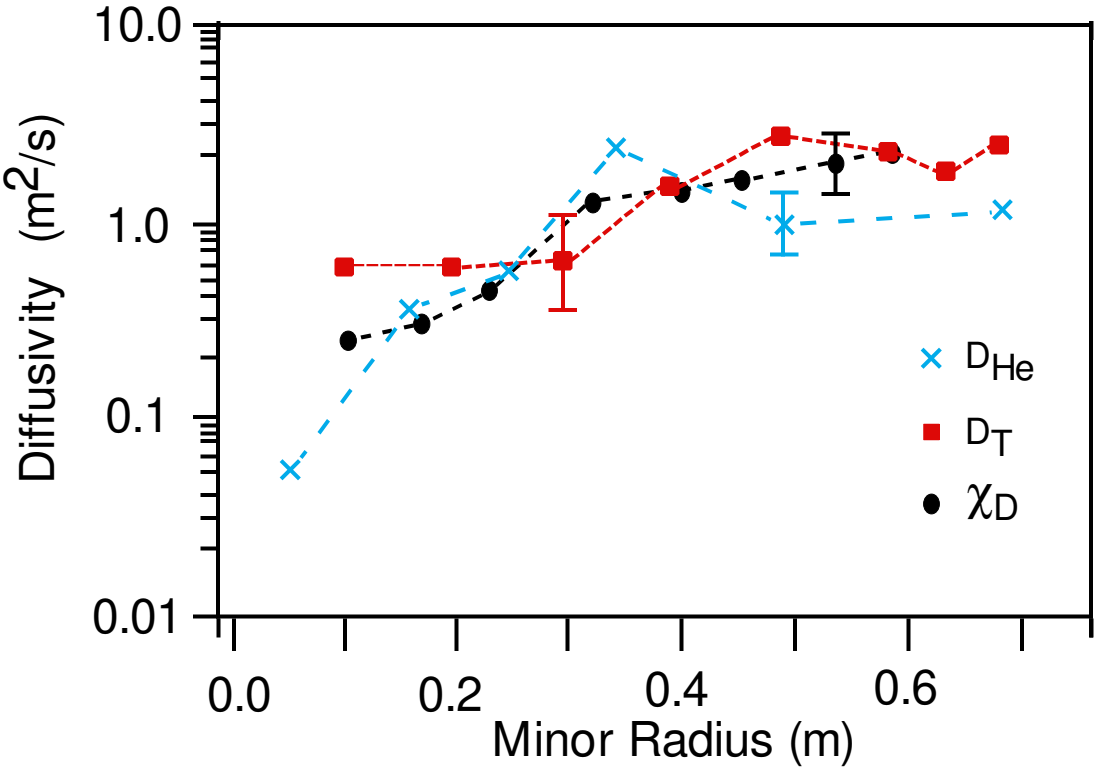

McG 94048